

High-energy physics image classification: A survey of Jet applications

Hamza Kheddar^a, Yassine Himeur^b, Abbas Amira^{c,d} and Rachik Soualah^e

^aLSEA Laboratory, Electrical Engineering Department, University of Medea

^bCollege of Engineering and Information Technology, University of Dubai, Dubai, UAE

^cDepartment of Computer Science, University of Sharjah, UAE

^dInstitute of Artificial Intelligence, De Montfort University, Leicester, United Kingdom

^eDepartment of Applied Physics and Astronomy, University of Sharjah, UAE

ARTICLE INFO

Keywords:

Jet images

High Energy Physics

Image classification

Deep learning

Machine learning

ABSTRACT

In recent times, the fields of **high-energy physics (HEP)** experimentation and phenomenological studies have seen the integration of **machine learning (ML)** and its specialized branch, **deep learning (DL)**. This survey offers a comprehensive assessment of these applications within the realm of various **DL** approaches. The initial segment of the paper introduces the fundamentals encompassing diverse particle physics types and establishes criteria for evaluating particle physics in tandem with learning models. Following this, a comprehensive taxonomy is presented for representing **HEP** images, encompassing accessible datasets, intricate details of preprocessing techniques, and methods of feature extraction and selection. Subsequently, the focus shifts to an exploration of available **artificial intelligence (AI)** models tailored to **HEP** images, along with a concentrated examination of **HEP** image classification pertaining to Jet particles. Within this review, a profound investigation is undertaken into distinct **ML** and **DL** proposed **state-of-the-art (SOTA)** techniques, underscoring their implications for **HEP** inquiries. The discussion delves into specific applications in substantial detail, including Jet tagging, Jet tracking, particle classification, and more. The survey culminates with an analysis concerning the present status of **HEP** grounded in **DL** methodologies, encompassing inherent challenges and prospective avenues for future research endeavors.

1. Introduction

HEP, also known as particle physics, is a fascinating and complex branch of science that delves into the fundamental constituents of the universe and the forces that govern their interactions. This field explores the smallest building blocks of matter and the nature of the physical laws that govern their behavior at incredibly high energies. At its core, **HEP** aims to understand the most basic elements of matter and the fundamental forces that shape the universe. It seeks to answer questions about the origins of the universe, the nature of dark matter and dark energy, the unification of fundamental forces, and the properties of particles that make up matter and energy. Researchers in this field utilize sophisticated tools and massive particle accelerators, such as the **large hadron collider (LHC)**, to probe matter at energy scales that are otherwise inaccessible. These colossal machines, which play a central role in **HEP**, accelerate subatomic particles to nearly the speed of light before colliding them, generating energy densities similar to those that existed just moments after the Big Bang. The collisions produced in these accelerators allow scientists to observe and study exotic particles that are often short-lived and can provide insights into the underlying structure of the universe.

The **standard model (SM)** of particle physics, which is the current theoretical framework in the field, describes the known elementary particles and their interactions. However, many mysteries remain unsolved, including the nature of dark matter, the absence of certain symmetries in the universe, and the lack of a unifying theory that reconciles gravity with the other fundamental forces. **HEP** has practical applications in technology and medicine, techniques and technologies developed in this field have led to advancements in medical imaging, radiation therapy, and materials science.

The data acquisition system of **LHC** stores the data on tape using grid computing, it can be disseminated for offline analysis aimed at extracting information concerning particle trajectories formed within the detectors. These trajectories contain concealed details about numerous particle characteristics. Computer vision techniques become relevant and play a crucial role during the analysis of offline data. Specifically, in the realm of **HEP** data analysis, **ML** algorithms have found success, leading to significant enhancements in event classification performance when contrasted with traditional methods rooted in expert understanding. Techniques like **boosted decision trees (BDT)**, shallow neural networks, and similar approaches have been employed in **HEP** data analysis. More recently, **deep neural network (DNN)** or **DL** have gained widespread adoption due to their applicability to intricate data structures such as images, videos, natural language, or sensor data. There are ongoing investigations into applying **DNNs** for analyzing granular details like particle positions and momentum as they traverse the detector. This has shown increased effectiveness in selecting signal events compared to **ML** algorithms employing conventional feature variables rooted in physics knowledge [1].

1.1. Motivation

In **HEP**, a *track* typically refers to the trajectory or path followed by a charged particle as it moves through a particle detector. **HEP** experiments often involve the collision of high-energy particles, such as those produced in particle accelerators like **LHC**. When these particles collide, they produce various other particles as a result of the interaction. These newly created particles then

* The first is the corresponding author.

✉ kheddar.hamza@univ-medea.dz (H. Kheddar); yhimeur@ud.ac.ae (Y. Himeur); aamira@sharjah.ac.ae, abbes.amira@dmu.ac.uk (A. Amira); yhimeur@ud.ac.ae (R. Soualah)

ORCID(s):

Table 1

Assessing how the proposed review aligns with previous research in the field of [HEP](#). The (✓) indicates that those specific areas have been addressed, whereas (✗) and (★) signify instances where certain areas have not been addressed, or partially addressed, respectively.

Reference	Paper type	Publication year	Jet Preliminaries	Taxonomy of HEP	Available Jet datasets	Jet images pre-proce.	Quantum ML for Jet images	DL models for Jet images	Jet image DL classif. techniques	Jet image DL apps	Research gaps and future direction
[2]	Mini review	2019	✗	✗	✗	✗	✗	✗	★	★	✗
[3]	Review	2021	✗	✗	✗	✗	✓	✗	✗	✗	★
[4]	Review	2021	★	✗	✗	✗	✗	★	★	★	★
[5]	Review	2022	✓	✗	✗	✗	✗	✗	✗	✗	✗
[7]	Review	2022	✓	✗	✗	★	✗	★	★	✗	✗
[6]	Review	2023	✓	✗	✗	✗	✗	✗	✗	✗	✗
Our	Review	2024	✓	✓	✓	✓	✓	✓	✓	✓	✓

pass through a series of detectors designed to measure their properties. Each charged particle leaves behind a trace or *track* as it interacts with the detector's various components, such as tracking chambers or silicon detectors. These tracks provide information about the particle's momentum, charge, and the path it took through the detector. Analyzing these tracks is crucial for understanding the physics of the collisions and for identifying the types of particles produced.

The reconstruction of particle tracks involves sophisticated algorithms and software that piece together the recorded data from various detector components to reconstruct the paths of the particles accurately. These reconstructed tracks are essential for a wide range of analyses in [HEP](#), including the discovery of new particles, the measurement of particle properties, and the investigation of fundamental forces and interactions in the universe.

However, in [HEP](#) experiments, there are always chances for high background signals or events that are not of primary interest to the experiment but can interfere with the detection and measurement of the particles or phenomena under investigation. The background sources could be the electronic components in the detector systems, when high-energy particles pass through matter, they can generate secondary particles through interactions, and others.

In the shade of the aforementioned phenomena and challenges, treating tracks / Jets in [HEP](#) as image-like data for processing and analysis is a useful approach, especially when dealing with the output from particle detectors. Hence, [ML](#) and [DL](#) play vital roles in [HEP](#) experiments. They serve the following purposes: i) Identifying and classifying particles by analyzing their tracks and energy deposits in detectors, thereby enhancing precision and identification speed. ii) Assisting in the accurate reconstruction of particle tracks from detector data, particularly in complex environments with numerous particles and interactions. iii) Enabling efficient data analysis, aiding researchers in sifting through extensive datasets to pinpoint rare or noteworthy events or particles. iv) Detecting anomalies or unexpected patterns in data, which could potentially signify the existence of new particles or physics beyond the [SM](#), among other applications. These contributions underscore the significance of [ML](#) and [DL](#) in advancing [HEP](#) research.

1.2. Related work

In recent years, there has been a surge in reviews addressing various aspects of [HEP](#) [2–6]. Review [2] delved into the realm of supervised deep learning applied to high-energy phenomenology, discussing specific use cases such as employing machine learning to explore new physics parameter spaces and utilizing graph neural networks for particle production and energy measurements at the [LHC](#). Meanwhile, paper [3] provided an overview of the initial forays into quantum machine learning in the context of [HEP](#) and offered insights into potential future applications. In [4], an array of novel tools relevant to [HEP](#) were introduced, complete with assessments of their performance, though there was limited discussion about future prospects. Lastly, the reviews [5, 6] comprehensively examined both theoretical and experimental aspects of Jets such as triggering, data acquisition systems, propagation, interactions, and related phenomena in [HEP](#).

Table 1 provided assesses how the proposed review aligns with previous research in the field of [HEP](#). Based on the assessment, it appears that our proposed review aims to comprehensively cover a wide range of topics in the field of [ML](#) and [DL](#)-based [HEP](#), including Jet preliminaries, taxonomy of [HEP](#), available Jet datasets, Jet image preprocessing, quantum machine learning, [DL](#) models for Jet images, classification techniques, Jet image [DL](#) applications, and research gaps/future directions. This suggests that the proposed review aims to provide a comprehensive overview of the current state of research in [HEP](#) and potential avenues for future work.

1.3. Contribution and survey structure

The objective of this survey is to provide a robust foundation for both [HEP](#) researchers aiming to grasp the principles of deep learning and its applications within the [HEP](#) domain, and for computer science researchers familiar with [AI](#) seeking insights into



Figure 1: Mind map of the proposed review.

the fundamental features and prerequisites essential for constructing a robust AI model tailored specifically for HEP, employing Jet images. To achieve this goal, our contribution is encapsulated in the following key points:

- The survey offers preliminary insights into the various types of particles and performance metrics associated with both AI-based and non-AI-based Jet particle physics methodologies.
- The taxonomy of ML and DL-based techniques in HEP for analyzing Jet images, along with their respective preprocessing and feature extraction methodologies, is thoroughly explored.
- The widely adopted AI models designed for analyzing HEP Jet images, along with their descriptive layered architectures, are extensively elaborated upon. Furthermore, their performance metrics are summarized and compared.
- Different state-of-the-art methods are clustered based on the AI techniques employed and comprehensively reviewed accordingly. Additionally, the exploration of AI-based applications in HEP Jet images is thoroughly detailed.
- Future directions and outlooks are explored, which aims to offer researchers insights into existing research gaps and areas within AI concepts and fields that remain unexplored in AI-based Jet images.

The structure of this paper is as follows: Section 2 presents the preliminaries necessary for understanding Jet images. In Section 3, the representation of Jet images in HEP is discussed. Section 4 provides a summary of the available AI models for analyzing HEP Jet images. Section 5 reviews AI-based methods for Jet images and categorizes them based on whether they employ ML or DL techniques. Section 6 showcases various AI-based applications of Jet images. Section 7 highlights the gaps and areas that remain unexplored in AI-based Jet image analysis, encompassing both techniques and applications. Finally, Section 8 concludes the survey.

2. Preliminaries

2.1. Types of particles

W and Z bosons: are important closely related particles described by the SM of particle physics. They and plays a significant role in the weak nuclear force, which is responsible for certain types of particle interactions and radioactive decay. The existence and properties of the Z boson, along with the W bosons, provided strong support for the electroweak theory and the SM as a whole. However, as with the W boson, the Standard Model has limitations and does not explain all aspects of particle physics, such as gravity, dark matter, and the hierarchy of particle masses. Here are some key points about the W and Z bosons:

- **Charge and Variants:** The W boson comes in two varieties: the W^+ and the W^- , which carry a positive and negative electric charge, respectively. These particles are antiparticles of each other. The Z boson is a neutral elementary particle.
- **Mass and Spin:** The W bosons masses are around $80.4 \text{ GeV}/c^2$ (gigaelectronvolts per speed of light squared). The Z boson has a relatively large mass. Its mass is around $91.2 \text{ GeV}/c^2$. Both W and Z bosons have a spin of 1, which is a measure of their intrinsic angular momentum.
- **Decay:** The W and Z bosons are unstable and have a very short lifetime. They quickly decay into other particles. For example, a W^+ boson can decay into a positron (an antielectron) and a neutrino, while a W^- boson can decay into an electron and an antineutrino. The Z can decay into various combinations of charged leptons (such as electrons and muons) and their corresponding antiparticles, as well as neutrinos and antineutrinos.

The Higgs boson: is crucial to our understanding of how other particles acquire mass and, by extension, how the universe's structure and behavior arise. The key points about the Higgs boson are:

- **Origin of Mass:** is associated with the Higgs field, a theoretical field that permeates all of space. In the **SM**, particles acquire mass by interacting with the Higgs field. The more a particle interacts with this field, the greater its mass will be. This mechanism explains why some particles are heavier than others.
- **Mass and Spin:** the Higgs boson itself has a mass of around $125.1 \text{ GeV}/c^2$. It has a spin of 0, which means it has no intrinsic angular momentum.
- **Decay:** is unstable and quickly decays into other particles after its creation in high-energy collisions. The specific decay modes and products depend on the energy at which it is produced.
- **Higgs field Interaction:** is a carrier of the interaction associated with the Higgs field. When particles move through space, they interact with this field, which gives them mass. The Higgs boson itself is the quantized excitation of this field.

The top quark: is one of the fundamental particles described by the Standard Model of particle physics. It holds a special place in particle physics due to its extremely large mass and its role in various processes involving high-energy collisions. Here are some key points about the top quark:

- **Mass:** The top quark is the heaviest known elementary particle. Its mass is approximately $173.2 \text{ GeV}/c^2$, which is even heavier than an entire atom of gold.
- **Quarks and the Strong Force:** Quarks are the building blocks of protons and neutrons, which are the constituents of atomic nuclei. The top quark, like all quarks, experiences a strong nuclear force, which is responsible for holding quarks together within hadrons (particles composed of quarks).
- **Weak Decays:** Due to its high mass, the top quark is relatively short-lived and decays before it can form bound states with other quarks to create hadrons. It decays primarily through weak interaction, one of the fundamental forces described by the Standard Model.
- **Production and Detection:** The top quark is typically produced in high-energy particle collisions, such as those that occur in experiments at particle accelerators like the **LHC**. Due to its high mass, the top quark is often produced along with its corresponding antiquark. Researchers detect its presence indirectly by observing its decay products, which can include other quarks, leptons (such as electrons and muons), and neutrinos.
- **Role in Electroweak Symmetry Breaking:** The top quark is of particular interest in theories related to electroweak symmetry breaking, a phenomenon that explains why certain particles acquire mass. Its large mass plays a significant role in the behavior of the Higgs boson and its interactions.

The b and \bar{b} Jets:

Jets composed of b and \bar{b} pairs are identified by mandating a minimum **transverse momentum** (p_T) of $20 \text{ GeV}/c$ for each jet and restricting their pseudorapidity (η) to the interval $2.2 < \eta < 4.2$. This criterion ensures the jets are well contained within the detector's instrumented region. Following initial selection, 16 distinct jet substructure features are utilized as inputs for the classification algorithms. Within a jet, the highest p_T muon, kaon, pion, electron, and proton are chosen. For each of these particles, three physical parameters are evaluated: the relative transverse momentum to the jet's axis (p_{rel}^T), the electric charge (q), and the separation in the (η, ϕ) space from the jet axis (ΔR). Should any particle type be absent, its corresponding features are assigned a value of 0. An additional characteristic, the weighted jet charge Q , is computed as the sum of the particles' charges inside the jet, each multiplied by its respective p_{rel}^T [8].

2.2. Performance measures

In the realm of **HEP**, performance assessment is divided into two main categories. The first encompasses classical metrics like energy loss, path length, and axis distance. The second involves metrics utilized are related to **DL**-based **HEP** techniques, such as accuracy, **true positive rate (TPR)**, **false-positive rate (FPR)**, **receiver operating characteristic (ROC)**, **area under curve (AUC)**, **mean squared error (MSE)**, **Fubini-study tensor (FST)**, among others. Table 2 outlines these metrics, including mathematical formulations and descriptions.

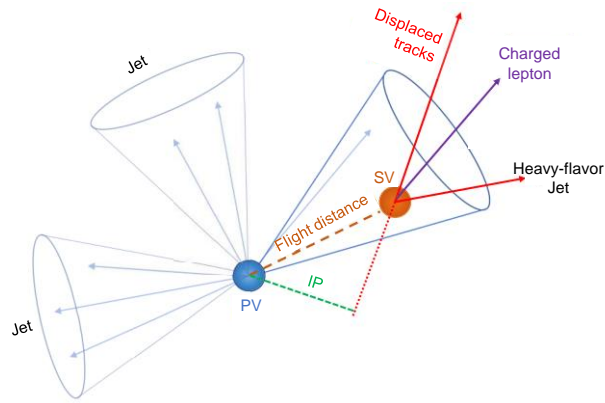


Figure 2: Visualization of decay involving a reconstructed jet and a secondary vertex, showcasing various noteworthy features [9].

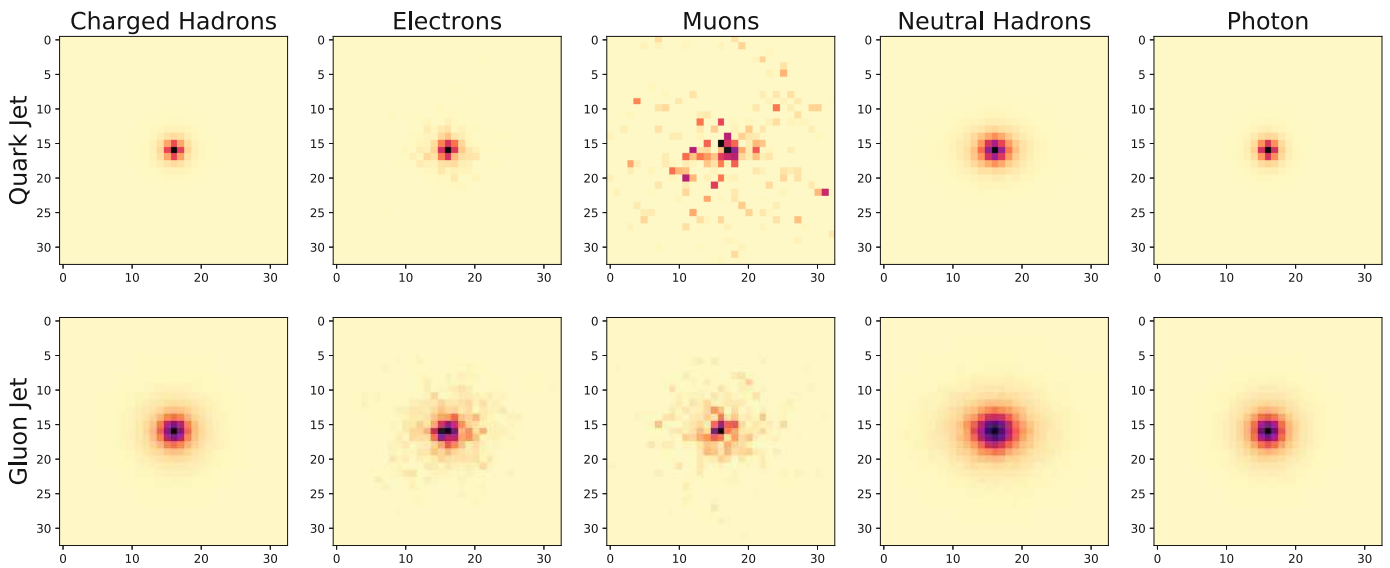


Figure 3: Jet images summed online and categorized into different channels employed in the analysis within the 100-200 GeV p_T range.

3. HEP Jet image representation

This section provides an overview of the Jet datasets comprising various forms of Jet images obtained and generated through different methods. Additionally, the current section delves into diverse pre-processing and feature extraction techniques employed in this context.

3.1. Available datasets

The [conseil Européen pour la recherche nucléaire \(CERN\)](http://opendata.cern.ch) open data portal provides access to a variety of datasets from experiments conducted at the Large LHC. These datasets include information about collisions, particles, and Jet images. The portal offers a great starting point for those interested in HEP datasets. Figure 3 illustrates samples of Jet images, featuring the average of p_T -normalized quark and gluon Jet images across 5 distinct χ bins. The Jet images may undergo different preprocessing techniques, discussed later, prior to input into ML/DL models for classification or prediction tasks. Table 3 showcases the datasets most commonly utilized in the reviewed research within this paper, including some generated datasets.

3.2. Pre-processing of Jet images

The objective of preprocessing input data is to support the model in addressing an optimization challenge. Usually, these preprocessing actions are not mandatory, but they are employed to enhance the numerical convergence of the model, considering the real-world constraints imposed by limited datasets and model dimensions, along with the specific parameter initialization choices.

¹<http://opendata.cern.ch/search?page=1&size=20&experiment=ATLAS>

²<https://opendata.cern.ch/search?page=1&size=20&q=jet%20images&experiment=CMS>

³<https://cp3.irmp.ucl.ac.be/projects/delphes>

⁴<http://madgraph.phys.ucl.ac.be/>

⁵<https://twiki.cern.ch/twiki/bin/view/CMSPublic/SWGuideFastSimulation>

⁶<https://zenodo.org/record/2603256>

⁷<https://archive.ics.uci.edu/dataset/280/higgs>

Table 2

An overview of the metrics employed to evaluate performance in particle physics.

Metric	Formula	Description	
Classic metrics	Energy loss ratio	$\chi_{jh} \equiv \frac{E_f^h}{E_i^h}$	determine, on a Jet-by-Jet basis, the amount of energy loss. The notation "jh" denotes the energy of the Jet at the hadronic scale. Here, E_f^h represents the p_T of a specific Jet when interacting with a medium, whereas E_i^h indicates the p_T of the identical Jet in the absence of any medium.
	Traversed path-length	$L = \frac{\sum_{i \in Jet} p_{T,i} L_i}{\sum_{i \in Jet} p_{T,i}}$	Offers significant insights closely related to the alterations and energy dissipation encountered by a Jet. This involves calculating the path length, L , traversed by a parton Jet, which is derived from the sum of the lengths of the Jet's constituents at the partonic level L_i , weighted by their p_T .
	Jet axis distance	$\Delta R = \sqrt{(\Delta\eta)^2 + (\Delta\phi)^2}$	The constituents of a Jet are predominantly confined within a conical shape, characterized by a separation from the Jet axis of $\Delta R = 0.5$. This separation ΔR encompasses both $\Delta\eta$, the variation in pseudo-rapidity, and $\Delta\phi$, the deviation in azimuthal angle relative to the Jet axis.
	Efficiency and Miss-efficiency rates	$Eff = \frac{N_{top}^{top}}{N_{top}}$, $Mistag = \frac{N_{QCD}^{top}}{N_{QCD}}$	Defining efficiency and mis-tag rates is crucial for assessing the performance of the Artificial Neural Network (ANN) tagger. Where N_{top} and N_{QCD} represent the total jet count in the top and QCD jet samples, respectively, and N_{top}^{QCD} signifies the number of jets in sample top tagged as type QCD .
Deep learning metrics	FPR and TPR	$\frac{FP}{FP + TN}$, $\frac{TP}{TP + FN}$	The FPR , is the ratio (or percentage) of the background signal that are incorrectly identified as containing Jet. The TPR , is the ratio (or percentage) of the Jet signal that is correctly identified as Jet (particle).
	AUC	$\int_0^1 TPR d(FPR)$	The area beneath the ROC curve is represented. It delivers a singular numeric score reflecting the cumulative effectiveness of the classification technique. An elevated AUC score signifies superior performance, with the ideal score being 1.
	Accuracy	$\frac{TP + TN}{TN + FN + TP + FP}$	The accuracy is the ratio (or percentage) of correctly detected instances of Jet in the signal. A high accuracy indicates that the classification algorithm is more effective in detecting Jet than background.
	MSE	$E(\theta) = \frac{1}{N} \sum_{i=1}^N (P_b^i(\theta) - T^i)^2$	The training procedure seeks to discover the model parameter values denoted as θ , which minimize the loss function known as MSE . Where N is the number of training Jets, P_b^i and T^i is the predicted and target probabilities, respectively, for the i -th Jet [8].
	F-measure	$2 \frac{\text{Precision} \times \text{Recall}}{\text{Precision} + \text{Recall}}$	Represents the harmonic mean between precision and recall metrics. This measure is applied to assess the comprehensive efficacy of the classification algorithm in identifying or tagging Jets.
	Joint and conditional distributions	$P(v \setminus O) \neq P(v) \quad \forall O$	If the probability distribution of the physics variable v , given the neural network output O , is influenced by the neural network output itself, then we interpret this as an indication that the network has acquired knowledge about this physics characteristic.
	FST	$\frac{1}{(1 + \sum_0^n z_n ^2)^2} \sum_{i=0}^n dz_i ^2$	The FST is an invariant metric tensor that can be used to describe distances between quantum states [10, 11]. z_i are complex coordinates, and $ dz_i $ represents the absolute value of the differential of z_i .
AMS	$\sqrt{2 \left((S + B + B_r) \ln \left(1 + \frac{S}{B + B_r} \right) - S \right)}$	The effectiveness of a method in categorizing test data into signal or background groups is assessed by employing approximate median significance (AMS) metric [4]. S is the sum of weights of true positives; B is the sum of weights of false positives; B_r is the regularization constant.	

In **HEP**, (i) η represents pseudorapidity, which is a measure related to the polar angle of a particle's trajectory. It is commonly used because it is less affected by relativistic effects and is approximately invariant under boosts along the beamline. (ii) ϕ represents the azimuthal angle, which is the angle around the beamline. (iii) Together, η and ϕ provide a way to specify the direction and position of particles or energy deposits within the detector. These coordinates are particularly useful for representing and analyzing the distribution of particles produced in high-energy collisions. (iv) The combination of η and ϕ can be thought of as a way to navigate and map the detector's components in a way that is sensitive to the underlying physics processes. (v) $\eta - \phi$ space is a coordinate system used to describe the properties and positions of particles or objects within particle detectors, particularly in experiments at large colliders like the **LHC**.

The subsequent sequence of data-driven preprocessing procedures was employed on the Jet images:

- **Center (translation and rotation):** Center the Jet image by translating it in (η, ϕ) coordinates, such that the pixel with the centroid weighted by total p_T is located at $(\eta, \phi) = (0, 0)$. This procedure involves rotating and boosting the Jet along the beam direction to position it at the center.
- **Crop:** Trim to a region of $value \times value$ pixels centered around $(\eta, \phi) = (0, 0)$, encompassing the area where η, ϕ fall within the range $(-R, R)$.
- **Normalize:** adjust the pixel intensities to ensure that the sum of all pixel values, $\sum_{i,j} I_{i,j}$, equals 1 across the image, with i and j serving as the pixel indices.
- **Zero-center:** Remove the average value, represented by $\mu_{i,j}$, from the normalized training set images from every image, thereby altering each pixel's intensity to $I_{i,j} = I_{i,j} - \mu_{i,j}$.

Table 3

 A summary of available data set and **event generator (EG)** for Jet HEP.

Dataset/EG	Name	Description	DLA ?
Dataset	ATLAS open data	Is one of the largest particle physics experiments at the LHC . They offer an "Open Data" initiative with datasets that include collision data and simulated samples. These datasets can be used to study Jet images and other particle physics phenomena.	Yes ¹
Dataset	CMS open data	Compact muon solenoid (CMS) is another major experiment at the LHC . Similar to ATLAS, CMS provides open data for educational and research purposes. The datasets include information about collisions, particles, and Jets.	Yes ²
EG	Delphes simulation	Is a particle physics event generator designed to produce simulated collision events that are similar to those observed in real experiments. It includes tools to generate Jet images based on the data produced in simulations.	Yes ³
EG	MadGraph	Is a popular event generator used in particle physics simulations. It can generate events involving Jets and other particles, which can then be turned into Jet images.	Yes ⁴
EG	FASTSim	Is a tool for simulating high-energy particle collisions. It can generate Jet images from simulated collision events and is often used for studying ML techniques in HEP .	Yes ⁵
Dataset	Complete [8]	It belongs to CERN and contains muon, kaon, pion, electron, and proton. In the complete dataset training, 400,000 Jets are used for training, and the remaining 290,000 are used for testing and assessing performance.	No
Dataset	Monte Carlo	It is generated through a dependable framework, created by integrating various tools like Pythia 8 for generating high-energy physics events, Delphes for emulating the detector's response, and RAVE for reconstructing secondary vertices. [12].	No
Dataset	Top tagging	This dataset comprises 1.2 million training samples, 400,000 for validation, and another 400,000 for testing. Each entry in this dataset corresponds to an individual Jet, with its source being either an energetic top quark, a light quark, or a gluon. These events were generated using the PYTHIA8 Monte Carlo event generator, and the response of the ATLAS detector is simulated using the DELPHES software package	Yes ⁶
Dataset	Quark-gluon tagging	The dataset is created by generating signal (quark) and background (gluon) Jets through PYTHIA8. For the signal Jets, the process involves $Z(\rightarrow \nu\nu) + (u, d, s)$, and for the background Jets, it uses $Z(\rightarrow \nu\nu) + g$. Notably, there is no simulation of the detector. The particles that are not neutrinos in the final state are grouped into Jets using the anti-kT algorithm with a radius parameter of $R = 0.4$. In total, this dataset contains 2 million Jets, evenly split between signal and background categories [13].	No
Dataset	Higgs dataset	The dataset originates from Monte Carlo simulations. The initial 21 attributes (found in columns 2-22) represent particle detector-derived kinematic properties within the accelerator. The remaining seven attributes are transformations of the initial 21, constituting high-level features engineered by physicists to aid in distinguishing between the two categories.	Yes ⁷
Dataset	QCD multi-Jet	Certainly! Here's the paraphrased version in LaTeX format: Samples are generated across different ranges of scalar sum of p_T , namely 1000-1500 GeV, 1500-2000 GeV, and 2000-Inf GeV. After excluding samples with p_T values less than 1000 GeV, the dataset consists of around $450 \cdot 10^3$ training images, $150 \cdot 10^3$ validation images, and $150 \cdot 10^3$ testing images [1].	No

 Abbreviations: [dataset link availability \(DLA\)](#).

- **Standardize:** Normalize each pixel by dividing it by $\sigma_{i,j}$ (the standard deviation) of the corresponding pixel value in the training dataset. This process is represented as: $I_{i,j} = I_{i,j}/(\sigma_{i,j} + r)$. A value of $r = 10^{-5}$ was employed to reduce the influence of noise.
- **Clustering and Trimming:** Reconstruct Jets by applying the anti- k_T algorithm [14] to all calorimeter towers, utilizing a specific Jet size parameter, such as $R = 1.0$, and then choose the primary (leading) Jet. Subsequently, refine the Jet by employing the k_T algorithm with a subjet size parameter of $r < R$, such as $r = 0.3$ [15].
- **Pixelisation:** Create a Jet image by discretizing the transverse energy of the Jet into pixels with dimensions (0.1, 0.1) in the $\eta - \phi$ space.
- **Zooming:** It is the option to magnify the Jet image by a factor that diminishes its reliance on the Jet's momentum.

3.3. Feature extraction and selection

Feature extraction and selection are important techniques in **HEP** for analyzing and interpreting data from experiments conducted at particle accelerators like the **LHC**. **HEP** experiments produce vast amounts of data, and the goal is to extract relevant characteristics from this data to make: (i) particles identifications, (ii) extract kinematic variables, such as p_T , energy (E), rapidity (y), and azimuthal angle (ϕ) for each detected particle, (iii) calculating the invariant mass of particle can reveal the presence of new particles, (iv) extract topological features related to the spatial distribution of particles or their interactions such as angular separations, impact parameters, and vertex finding. The benefit of feature selection is to make: (i) dimensionality reduction techniques like **principal component analysis (PCA)** or **t-distributed stochastic neighbor embedding (t-SNE)** may be employed to reduce the number of features while retaining as much information as possible, (ii) identify the most discriminating features that separate signal from background, (iii) identify the most relevant features for **ML** classification and model building.

Di Luca et al. [12] presents an automated feature selection procedure for particle Jet classification in **HEP** experiments. The authors use **ML** boosted tree algorithms to rank the importance of observables and select the most important features associated

Table 4

Possible combinations of Jet features to generate new high- and low-level features that could potentially improve ML classification for Jet HEP. The performance of employing these features are in [16].

Level	Suggested feature name	Description	Grouping
High-level features	DER_mass_MMC	The Higgs boson's mass was estimated using a hypothesis-driven fitting method.	Higgs, Mass
	DER_mass_transverse_met_lep	Transverse mass associated with the lepton and P_{miss}^T	Higgs, Mass
	DER_mass_vis	The mass invariant to both the lepton and the tau	Higgs, Mass
	DER_pt_h	Transverse momenta of the combined vector of the lepton, tau, and P_{miss}^T	Higgs, 3-momenta
	DER_deltaeta_jet_jet	Absolute disparity in pseudorapidity between the leading and subleading jets (undefined for less than two jets)	Jet with angular properties
	DER_mass_jet_jet	The invariant mass of the primary and secondary jets (not applicable when there are fewer than two jets).	Jet, Mass
	DER_prodelta_jet_jet	The multiplication of the pseudo rapidities for the foremost and next-to-foremost jets (inapplicable if fewer than two jets are present).	Jet, 3-momenta
	DER_deltar_tau_lep	Distance between the lepton and the tau in the $\eta - \phi$ plane.	Final state, Angular
	DER_pt_tot	The p_T resulting from the vector addition of the p_T of the lepton, tau, the primary and secondary jets (when applicable), and P_{miss}^T .	Final-state, Sum
	DER_sum_pt	Total transverse momentum of the lepton, tau, and all jets	global event, Sum
	DER_pt_ratio_lep_tau	Ratio of the transverse momenta of the lepton to that of the tau	Final state, 3-momenta
	DER_met_phi_centrality	Centrality of the azimuthal angle of P_{miss}^T relative to the lepton and the tau	Final state, Angular
DER_lep_eta_centrality	The centrality measure of the lepton's pseud-orapidity in comparison to the primary and secondary jets (not applicable for fewer than two jets).	Jet, Angular	
Low-level features	PRI_tau_[px/py/pz]	The 3-momenta of the tau expressed in Cartesian coordinates.	Final state, 3-momenta
	PRI_lep_[px/py/pz]	The lepton's 3-momenta represented in Cartesian coordinates.	Final state, 3-momenta
	PRI_met_[px/py]	The constituent parts of the missing transverse momentum vector expressed in Cartesian coordinates.	Final state, 3-momenta
	PRI_met	The magnitude of the missing transverse momentum vector represented in Cartesian coordinates.	Final state, 3-momenta
	PRI_met_sumet	Total sum of transverse energy.	Final-state, Energy
	PRI_jet_num	Count of jets present in the event.	Jet, Multiplicity
	PRI_jet_leading_[px/py/pz]	The three-dimensional momenta of the primary jet expressed in Cartesian coordinates (not applicable if there are no jets present).	Jet, 3-momenta
	PRI_jet_subleading_[px/py/pz]	The 3-momenta of the secondary jet represented in Cartesian coordinates (not defined if fewer than two jets are present).	Jet, 3-momenta
	PRI_jet_all_pt	Total sum of the transverse momenta of all jets in Cartesian coordinates.	Jet, 3-momenta

Note: PRI_jet_all_pt may diverge from the sum of the transverse momenta of the leading and subleading jets because events can feature more than two jets.

with a particle Jet. They apply this method to the specific case of boosted Higgs boson decaying to two b-quarks ($H \rightarrow bb$) tagging and demonstrate the impact of feature selection on the performance of the classifier to distinguish these events amidst the substantial and unalterable background originating from quantum chromodynamics (QCD) multi-Jet production. They also train a fully connected neural network to tag the Jets and compare the results obtained using all the features or only those selected from the procedure which consists of two main steps: data preparation and feature ranking extraction. The authors discover that the azimuthal angles of the large-R Jet and the variable radius (VR)-track Jets appear towards the end of the feature ranking. At the top of the ranking, they find the p_T of the two VR-track Jets, along with certain details regarding the secondary vertex, such as its mass, energy, and displacement. The study shows that selecting the highest-ranked features achieves performance nearly as effective as that of the full model, with only a slight deviation of a few percent. This approach can be expanded to accommodate the increased number of observable variables that upcoming collider experiments will gather from high p_T particle Jets. The data for this research comes from proton-proton collision events featuring a boosted Higgs boson that decays into two b quarks. In [16], solutions have been proposed for classifying events extracted from the 2014 Higgs ML Kaggle dataset⁸. The dataset includes a mix of low-level and high-level attributes: it contains 18 low-level features that include three-dimensional momenta (p_T , η , ϕ), missing transverse momentum, and the total transverse momentum from all jets; additionally, there are 13 high-level features motivated by physics, covering invariant masses and angular separations among objects in the final state. Table 4 summarizes the features utilized, which hold potential for future application within the context of HEP. The authors' aim to ensure that the suggested networks make effective use of low-level information; otherwise, there's a risk of losing these features during selection. Their focus lies in determining the necessity of high-level features. The proposed DNN model effectively utilize the low-level information in the data and autonomously learn their own high-level representations. Boost-invariant polynomial (BIP) features are a type of mathematical representation used in HEP for analyzing particle collision data. They are constructed to be invariant under boosts, meaning they remain unchanged under transformations to different reference frames with different velocities. These features are designed to capture important characteristics of particle jets, such as their energy distribution and substructure, while ensuring consistency across various experimental conditions. BIP features are particularly useful for tasks like jet tagging and classification in HEP experiments, as employed in [17].

4. Available AI models for HEP Jet images

Many DL architectures have been proposed in the SOTA of HEP domain to identify particles, Table 5 summarizes and compares the most efficient DL models, used in HEP, based on their architectures and performances. For example, the work in [18] proposed PartT, which is a new Transformer-based architecture for Jet tagging. Its main task is to identify the origin of a Jet of particles

⁸<https://www.kaggle.com/c/higgs-boson>

produced in HEP experiments. ParT makes use of two sets of inputs: (i) the particle input, which includes a list of features for every particle and forms an array, and (ii) the interaction input, which is a matrix of features for every pair of particles. ParT employs a novel **pairwise multi-head attention (P-MHA)** mechanism, which allows the model to attend to pairs of particles and learn their interactions. The P-MHA is more effective than standard plain multi-head attention. This assertion is substantiated when the pre-trained ParT models are fine-tuned on two widely adopted Jet tagging benchmarks, the quark-gluon tagging dataset and the binary classification dataset for identifying boosted W bosons decaying to two quarks. The fine-tuning process involves training the ParT models on a smaller labeled dataset specific to each benchmark, which allows the models to learn the specific features and patterns relevant to each task. The fine-tuned ParT models achieve significantly higher tagging performance than the models trained from scratch and outperform the previous SOTA models, including ParticleNet and other Transformer-based models.

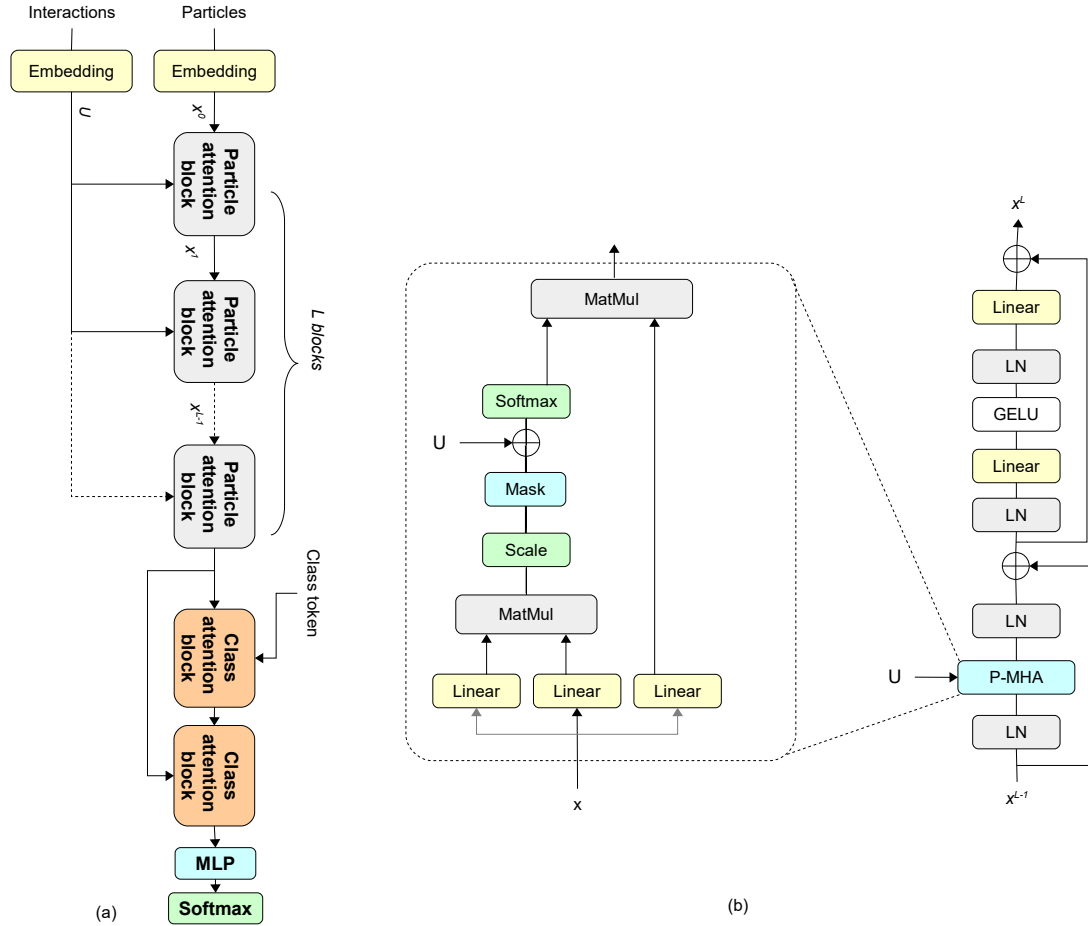


Figure 4: The architecture of partT model suggested in [18]. (a) Particle Transformer; (b) Particle attention block.

Another architecture called the LorentzNet is proposed in [13], which is based on the **Lorentz group equivariant block (LGEb)** block. The structure of LGEb consists of several layers, including Minkowski norm and inner product, sum pooling, a **multi-Layer perceptron (MLP)**, and a Clebsch-Gordan tensor product. The input of LGEb is a set of 4-momentum vectors, which are transformed by the Minkowski norm and inner product layer to obtain Lorentz-invariant geometric quantities. The sum pooling layer aggregates the geometric quantities to obtain a scalar representation of the input. The MLP layer is used to learn a nonlinear mapping from the scalar representation to a new feature space. Finally, the Clebsch-Gordan tensor product layer is used to combine the new feature space with the original input to obtain the output of LGEb. It is designed as a Lorentz group-equivariant mapping to preserve the symmetries of the Lorentz group, ensuring the model's equivariance and universality.

Unlike the previous models, the authors in [19] proposed the **equivariant graph neural networks (EGNN)** model, which is a **graph neural network (GNN)** architecture that is translation, rotation, and reflection equivariant ($E(n)$), and permutation equivariant with respect to an input set of points. It uses a set of filters that are equivariant to the action of the symmetry group, which are constructed using a combination of radial basis functions and Chebyshev polynomials. The EGNN can retain the flexibility of GNNs while remaining $E(n)$ equivariant as the radial field algorithm and without the need to compute expensive operations (i.e. spherical harmonics). The EGNN outperforms other equivariant and non-equivariant alternatives while still being efficient in terms of running time. Besides, EGNN reduces the error with respect to SOTA method by 32%.

Similarly, [20] proposed the ParticleNet model. The architecture is a customized neural network that operates directly on particle clouds for Jet tagging. It uses dynamic graph **convolutional neural networks (CNNs)** to process the unordered set of constituent particles that make up a Jet. The architecture consists of three EdgeConv blocks, each with a different number of channels and nearest neighbors. EdgeConv block starts by representing a point cloud as a graph, whose vertices are the points themselves, and

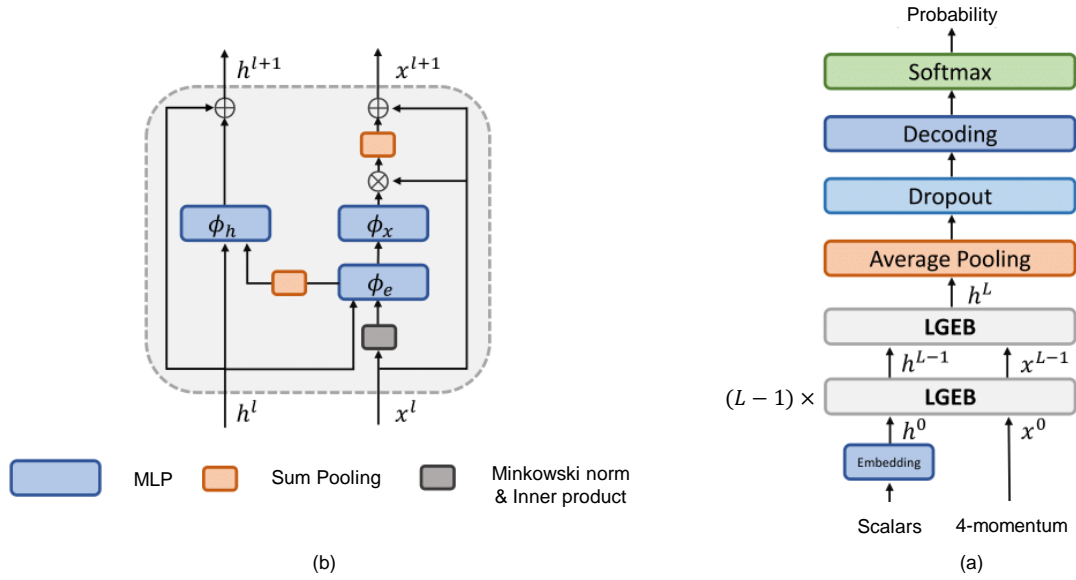


Figure 5: (a) The architecture of LorentzNet model. (b) LGEB block [13].

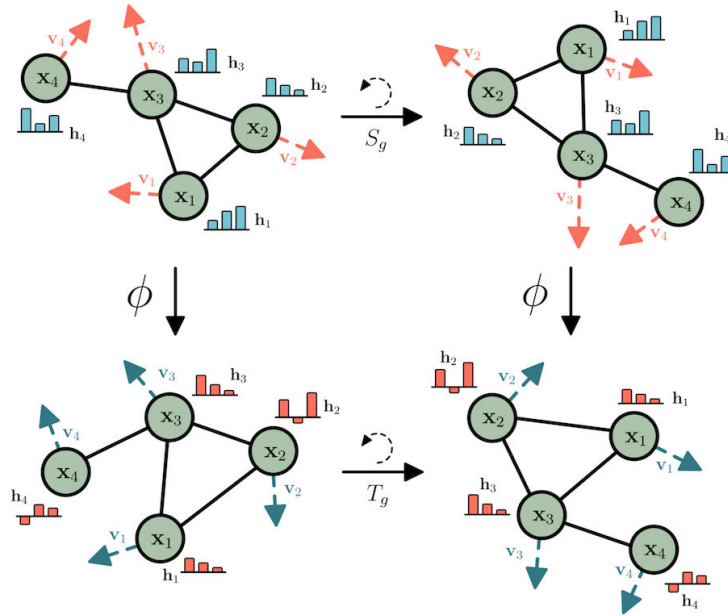


Figure 6: The architecture of EGNN model suggested in [19].

the edges are constructed as connections between each point to its **K-nearest neighbors (KNN)** points. The EdgeConv block then finds the **KNN** particles for each particle, using the "coordinates" input of the EdgeConv block to compute the distances. Inputs to the EdgeConv operation, the "edge features," are constructed from the "features" input using the indices of **KNN** particles. The EdgeConv procedure is executed using a three-layer **MLP**. Each layer is structured to include a linear transformation, succeeded by batch normalization, and subsequently a **rectified linear unit (ReLU)** activation. Additionally, a shortcut connection is integrated into every block parallel to the EdgeConv operation, facilitating the direct passage of input features. An EdgeConv block is defined by two key hyper-parameters: the neighbor count k and the channel count C , which respectively denote the number of neighbors to consider and the number of units within each layer of linear transformation. The EdgeConv blocks play a crucial role in learning the local features of the particle cloud and aggregating them into a global feature vector for the Jet. Following EdgeConv blocks, global average pooling aggregates particle features, leading to a 256-unit fully connected layer, **ReLU** activation, dropout, and a 2-unit softmax output for binary classification. The ParticleNet architecture achieves **SOTA** performance on two representative Jet tagging benchmarks and is improved significantly over existing methods.

The paper [21] introduces the **Lorentz group network (LGN)** neural network model designed for particle physics identification. This model is characterized by its full equivariance to transformations under the Lorentz group, which represents a crucial symmetry of space-time in physics. The **LGN** model is designed to simplify models, reduce the number of learnable parameters, and gain a deeper understanding of the physical interpretation of results. The model is based on the tensor product of representations of the

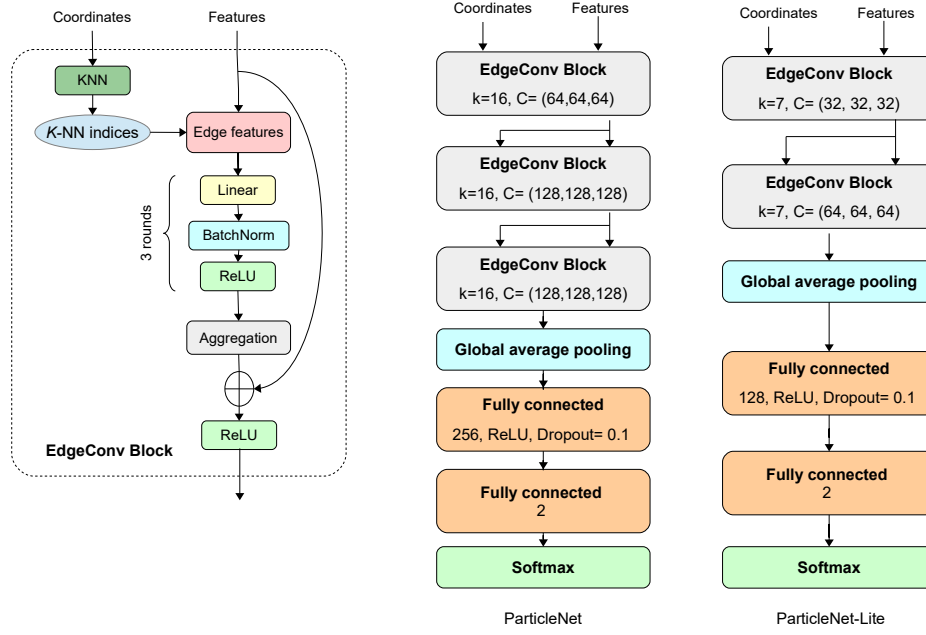


Figure 7: The architecture of ParticleNet model suggested in [20].

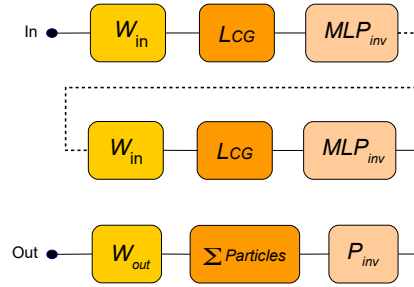


Figure 8: The architecture of LNG model suggested in [21].

Lorentz group, which allows for equivariant nonlinearity. The **LGN** architecture has been successfully applied to a classification task in particle physics called top tagging, whose objective is to distinguish top quark "Jets" from a backdrop of lighter quarks. The **LGN** model consists of several layers, including the linear input layer (W_{in}), iterated **Clebsch-Gordan (CG)** layers (L_{CG}), and perceptrons MLP_{inv} layer. The initial linear layer processes the 4-momenta of N_{obj} particles originating from a collision event, and it can also handle associated scalar quantities like label, charge, spin, and more. The iterated L_{CG} layers are defined by a **CG** decomposition of the tensor product of representations of the Lorentz group, which allows for equivariant non-linearity. The **CG** layers are alternated with perceptrons MLP_{inv} layer, which act only on Lorentz invariants. At the end of each **CG** layer, a **MLP** is applied to the isotopic component of the tensor product. The **MLP** accepts $N_{ch}^{(p)}$ scalar inputs and generates an equivalent number of outputs, with its parameters uniformly applied across all N_{obj} nodes within the **CG** layer. The output layer computes the arithmetic sum of the activations from N_{obj} and extracts the invariant isotopic aspect of this sum. It subsequently employs a final fully connected linear layer, denoted as W_{out} , on the $N_{ch}^{(NCG)}$ scalars, generating two scalar weights for binary classification. In the **LGN** model's output layer, P_{inv} conducts the projection onto invariants, combines contributions from particles to ensure permutation invariance and subsequently applies a linear transformation. P_{inv} operates independently on each individual particle but maintains consistent parameter values across all particles. The **LGN** model has demonstrated competitive performance while using between 10-1000 times fewer parameters than other **SOTA** models.

Another **DL** architecture called the DeepJet model, designed to consider the full information of all Jet constituents, including secondary vertices, global event variables, and charged and neutral particles, simultaneously, is proposed in [22]. The model architecture consists of several components: (i) Automatic feature extraction is conducted for each constituent through convolutional branches that include 1×1 convolutional layers. Distinct convolutional branches are allocated for vertices, charged particle flow candidates, and neutral particle flow candidates. (ii) The output of the convolutional branches is used to construct a graph representation of the Jet, where each constituent is represented as a node in the graph. The edges between the nodes are determined by a distance metric that takes into account the kinematic properties of the constituents. (iii) The graph representation of the Jet is then processed by several graph convolutional layers, which are designed to capture the correlations between the constituents. The graph convolutional layers use a learnable filter that is applied to the graph representation of the Jet. (iv) The output of the graph convolutional layers is then fed into several dense layers, which are designed to perform the final classification task. The

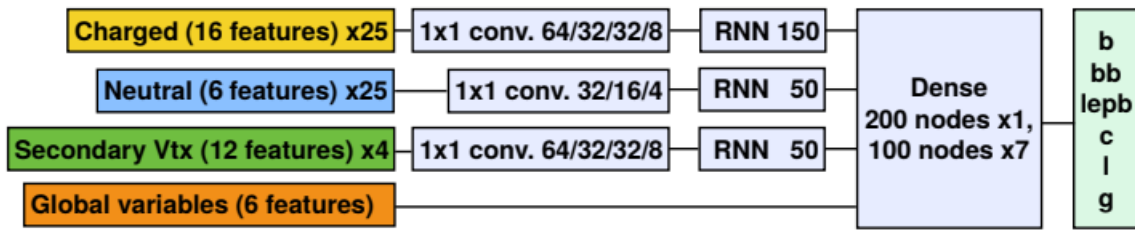


Figure 9: The architecture of DeepJet model suggested in [22].

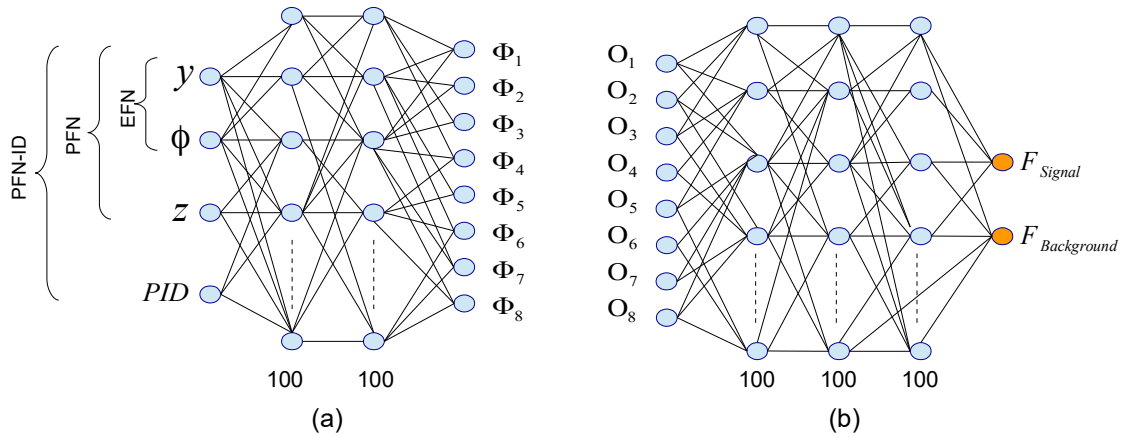


Figure 10: The architecture of PFN-ID model suggested in [23]. (a) Per-particle mapping Φ . (b) The binary output signal or background can be identified.

dense layers use a combination of fully connected and batch normalization layers. In the context of the DeepJet model, the **recurrent neural network (RNN)** layer is an important component of the DeepJet model, as it allows the model to capture the sequential information in the charged particle tracks and to use this information to improve the classification performance. The DeepJet model has been shown to achieve **SOTA** performance in Jet flavour classification and quark/gluon discrimination tasks. The model was tested using **CMS** simulation and was found to outperform previous classifiers, including the IP3D algorithm. The DeepJet model underwent a comparative analysis against a binary quark/gluon classifier from the **CMS** reconstruction framework. An improvement in performance was noted with the use of the DeepJet model on a dataset comprised exclusively of light quark and gluon Jets. Moreover, the DeepJet model was found to be more robust to variations in the Jet constituents and kinematics, which makes it more suitable for use in real-world scenarios. In terms of DeepJet's Performance, using the function of reconstructed vertices, b-Jet efficiency can reach 92%, and when the function of Jet p_T , b-Jet efficiency is around 95%.

Particle flow network with ID (PFN-ID) model [23] is another proposed type of **ML** architecture that takes particles as input and processes them in a way that is dependent on the order the particles were fed into the network. The **PFN-ID** architecture is based on the Deep Sets framework and includes full particle ID information. The Deep Sets framework is a **ML** approach that allows for learning directly from sets of features or "point clouds". The following are the main steps of the framework: (i) Map each element of the set to a latent space using a shared function. (ii) Aggregate the latent representations of the elements using a symmetric function. (iii) Map the aggregated latent representation back to the output space using a shared function. The framework guarantees that a generic symmetric function can be represented by an additive latent space. In the context of particle-level collider observables, each particle is mapped to a latent representation and then summed over, and observables are then functions on that latent space. This decomposition encompasses a wide variety of existing event- and Jet-level collider observables and representations, including image-based and moment-based methods. The **PFN-ID** improves the classification performance of the **particle flow network (PFN)** model for discriminating quark and gluon Jets. Results show that **PFN-ID** slightly outperforms **RNN-ID**, whereas the **PFN** and **RNN** are comparable.

The **CNN** tagger architecture proposed in the paper [24] consists of a **CNN** with four identical convolutional layers, each with 8 feature maps and a 4×4 kernel. These layers are separated in half by one 2×2 max-pooling layer. The **CNN** also includes three fully connected layers of 64 neurons each and an output layer of two softmax neurons. Zero-padding is included before each convolutional layer to prevent spurious boundary effects. The architecture ends with a flatten layer and three fully connected layers with sizes 64, 256, 256, and 2, respectively. The **CNN** is trained on a total of 150k+150k top and **QCD** Jet images, by minimizing a **MSE** loss function using the stochastic gradient descent algorithm in mini-batches of 1000 Jet images and a learning rate of 0.003.

The **TopoDNN** model proposed in [25] is a **DNN**-based architecture. The network's input layer is designed to process vectors containing the Jet constituents' p_T , η , and ϕ values. Manual tuning of the network's architecture involved adjusting the depth and node count per layer, within a range of 4-6 layers and 40-1000 nodes per layer, respectively. **ReLU** activation function was implemented in the hidden layers, whereas a sigmoid function was applied to the output node. The training process utilized the Adam optimizer, with training sessions capped at a maximum of 40 epochs. An early stopping mechanism was employed, utilizing

High-energy physics image classification: A survey of Jet

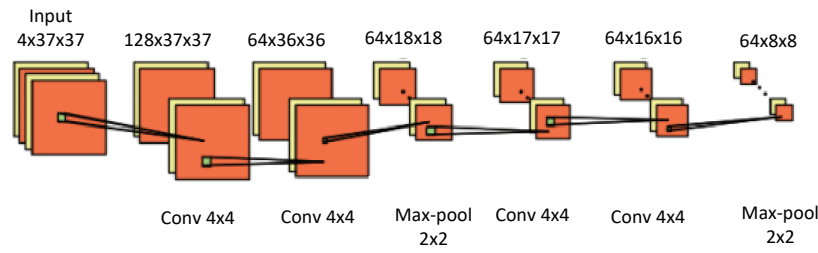


Figure 11: The architecture of CNN tagger model suggested in [24].

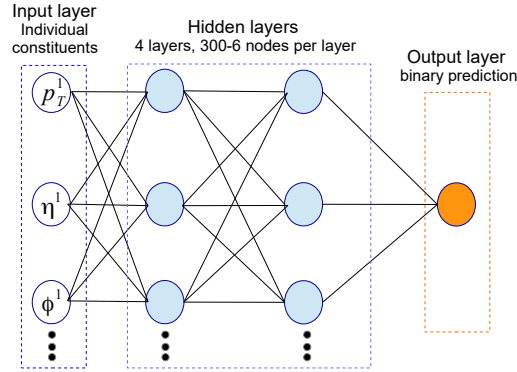


Figure 12: The architecture of TopoDNN model suggested in [25].

Table 5

A summary of available DL architectures for Jet HEP classification.

Ref.	Year	Model	Performance TT		Performance QG		Other performance		Link
			Acc.	AUC	Acc.	AUC	Acc.	AUC	
[18]	2022	partT	0.944	0.9877	0.852	0.9230	–	–	Yes ⁹
[13]	2022	LorentzNet	0.942	0.9868	0.844	0.9156	–	–	No
[19]	2021	EGNN	0.922	0.9760	0.803	0.8806	–	–	Yes ¹⁰
[20]	2020	ParticleNet	0.940	0.9858	0.840	0.9116	–	–	No
[21]	2020	LGN	0.929	0.9640	0.803	0.8324	–	–	Yes ¹¹
[23]	2019	PFN-ID	0.932	0.9819	0.9005	–	–	–	No
[24]	2018	CNN tagger	–	–	–	–	0.87 (DTJ) 0.945 (CJ)	0.943 (DTJ) 0.988 (CJ)	No
[25]	2017	TopoDNN	0.916	0.972	–	–	–	–	No

Abbreviation: TT: Top tagging; QG: Quark-gluon; DTJ: DeepTop Jets; CJ: CMS Jets:

a patience parameter set to 5 epochs based on the validation set loss. The final architecture selected features 4 hidden layers, comprising 300, 102, 12, and 6 nodes in each layer respectively. TopoDNN achieved a significant background rejection of 45 at a 50% efficiency operating point for reconstruction-level Jets, yielding to correctly identify top quark Jets with a high level of accuracy while rejecting a large portion of background events.

5. HEP Jet image classification

ML, especially neural networks, has a rich historical presence in the field of particle physics. The concept of applying neural networks for tasks like distinguishing quarks and gluons, tagging Higgs particles, and identifying particle tracks has been around for more than two and a half decades. Nevertheless, the recent advancements in deep learning and the increased computational capabilities offered by [graphics processing units \(GPUs\)](#) have led to a significant enhancement in image recognition technology. As a result, there has been a renewed and heightened interest in utilizing these techniques. In the subsequent sections, we provide an overview of [SOTA](#) methods in both [ML](#) and [DL](#). Figure 13 depicts a taxonomy of existing [ML](#) and [DL](#) techniques (discussed in Section 5), summarizes the previously discussed AI-based Jet images models (discussed in Section 4), preprocessing and datasets (discussed in Section 3), and metrics (discussed in Section 2).

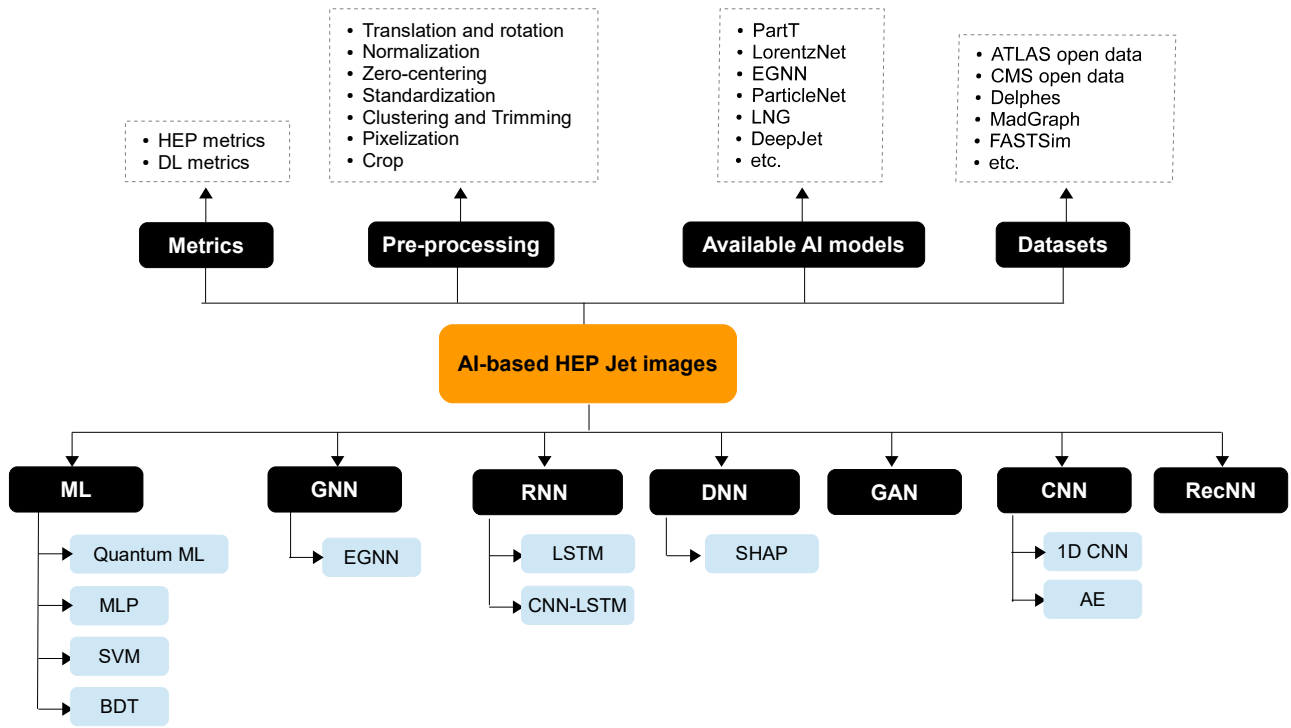


Figure 13: Taxonomy of ML and DL-based HEP techniques for Jet images, with associated preprocessing, metrics, and datasets.

5.1. Quantum ML-based

ML-based analysis of HEP Jet images has become an important technique in recent years. Jets are collimated sprays of particles, i.e. emitted from a source in a way that they are parallel or nearly parallel to each other, produced in high-energy particle collisions. Analyzing their properties is crucial for understanding the underlying physics processes. Jet images are essentially 2D representations of the energy distribution within a Jet, where each pixel corresponds to a small region of the Jet. quantum machine learning (QML) methods have recently found applications in addressing challenges within HEP, including separating signal from background [10], detecting anomalies [26], and reconstructing particle tracks [27].

The paper [28] discusses the potential applications of quantum computation and QML in HEP, rather than focusing on deep mathematical structures. The authors claim that statistical ML methods are used for track and vertex reconstruction. These methods vary depending on the detector geometry and magnetic field used in the experiment. ML can help address these challenges by providing efficient and accurate methods for pattern recognition and particle identification. They suggest that quantum algorithms could potentially improve upon existing methods by offering faster and more efficient solutions to challenging problems in experimental HEP, such as particle identification and track reconstruction. This can be realized by creating a dataset recorded on tape through grid computing, which can be distributed for offline analysis using QML to extract information about particle trajectories developed inside the detectors.

Similarly, the researchers in [8] present a new approach to Jet classification using QML. The method involves embedding data into a quantum state, passing it through a variational quantum circuit, and performing a training procedure by minimizing a classical loss function. Probability measurements of the final state are then used to perform the classification. By exploiting the intrinsic properties of quantum computation, such as superposition and entanglement, the team aims to identify if a Jet contains a hadron formed by a b or \bar{b} quark at the moment of production. The approach could lead to new insights and enhance the classification performance in particle physics experiments. Two datasets have been used in this research: the complete dataset and the muon dataset, both of which belong to CERN. In the muon dataset analysis, 60,000 Jets are used for training and 40,000 Jets are used for testing. The muon dataset is a subset of the complete dataset, and it is used to evaluate the dependence of the quantum algorithms' performance on the number of training events and the circuit complexity. The researchers compare the performance of their QML approach with that of DNN, long short-term memory (LSTM), and LSTM with convolutional layer models. They show that the results for tagging power as a function of the Jet p_T and η are comparable within the MSE error, and therefore, they consider only the DNN model for comparison with QML algorithms. Blance and Spannowsky [10] proposed a hybrid variational quantum classifier that combines quantum computing methods with classical neural network techniques to improve classification performance in particle physics research. The algorithm is applied to a resonance search in di-top final states, and it outperforms both classical neural networks and QML methods trained with non-quantum optimization methods. The classifier's ability to be trained on small amounts of data indicates its potential benefits in data-driven classification problems. The proposed methodology was applied to the generated dataset, and the hybrid approach using the FST metric outperformed both classical neural networks and QML methods trained with non-quantum optimization methods in terms of maximizing learning outcomes; its accuracy can reach 72.6%. The hybrid approach also learned faster than an equivalent classical neural network or the classically trained variational quantum classifier. The work

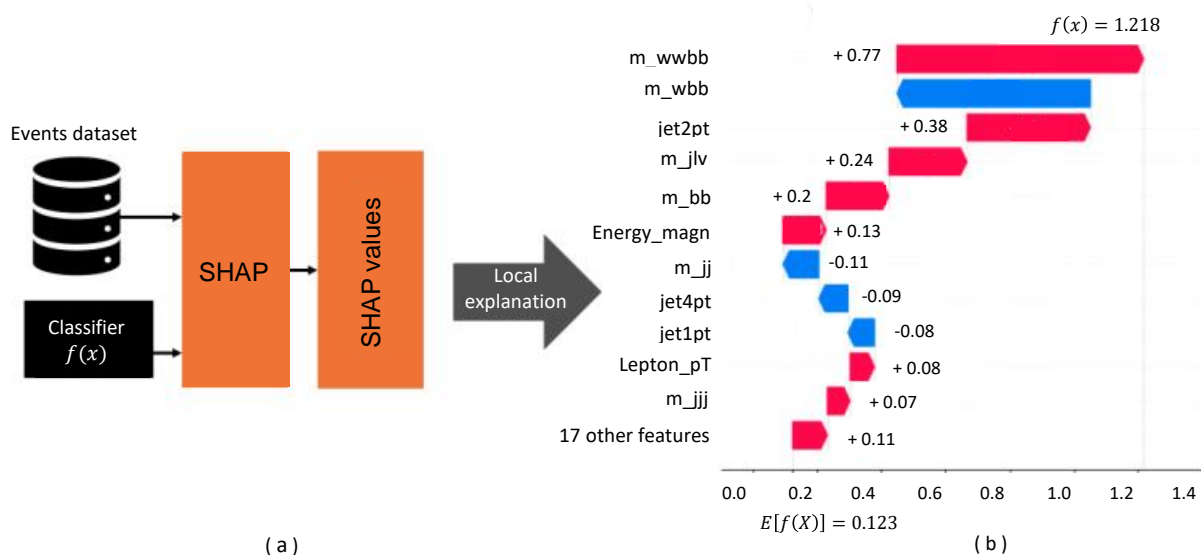


Figure 14: (a) Diagram illustrating the localized explanation of an event classifier with the SHAP method. (b) Localized SHAP explanation represented using a waterfall plot. It can be observed that the SHAP values are associated with individual event features. The classifier's prediction (XGBoost) is $f(x) = 1.218$, while the base value is $E[f(x)] = 0.123$. In this context, the feature "m_wvbb" contributes positively with a SHAP value of +0.77, increasing the prediction, whereas the feature "m_wbb" has a SHAP value of -0.6, reducing the prediction.

[29] investigates the potential of QML in HEP analysis at the LHC. The authors compare the performance of the quantum kernel algorithm to classical ML algorithms using 15 input variables and up to 50,000 events. They used 60 statistically independent datasets of 20,000 events each for their analysis. The AUC is used as the metric, and the results show that the performance of all methods improves with increasing dataset size. For 15 qubits, the quantum SVM-Kernel algorithm performs similarly to the classical support vector machine (SVM) and classical BDT algorithms. The quantum SVM-Kernel performances from the three different quantum computer simulators (Google, IBM, and Amazon) are comparable. The authors also claim that when a selection is implemented, permitting a signal acceptance rate of 70%, it results in the rejection of approximately 92% of background events, as indicated by the AUC. Consequently, the S/\sqrt{B} ratio will experience an enhancement of approximately 150% compared to a scenario without any selection.

5.2. DNN-based

The DNNs are a type of artificial neural network that are composed of multiple layers of nodes, with each node connected to every node in the previous and next layers. They are particularly well-suited for processing high-dimensional data, such as images or collections of features, and can learn complex non-linear relationships between inputs and outputs. In the context of HEP, the DNN was used in to classify hadronic Jets based on their input features. DNNs typically require a fixed-size input, which can be a limitation when working with variable-length inputs such as particle lists.

In [30], DNNs are used in HEP to classify Jets produced in particle collisions. DNNs can automatically extract features from Jet images, allowing for more accurate classification than traditional methods that rely on expert-designed features. However, the authors in [23] used DNNs to process collections of ordered inputs, which can be thought of as a fixed-size representation of variable-length inputs. This allows the DNN to learn features sensitive to particle ordering, which can be important for discriminating between different types of Jets. The study [31] applies the shapley additive explanations (SHAP) method to explain the output of two HEP events DNN classifiers (and XGBoost) using the Higgs dataset. It demonstrates SHAP's utility in understanding complex ML systems, particularly in the context of HEP event classifiers. The TreeExplainer and DeepExplainer methods from the Python SHAP library were used to compute SHAP values, revealing that features like m_{bb} , m_{wvbb} , and m_{wbb} were crucial in both models, although their distribution of SHAP values differed, indicating distinct learning processes. The process of extracting SHAP values are depicted in Figure 14.

The identification of b Jets using QCD-inspired observables was studied in [32]. It involves the application of Jet substructure observables, such as one-dimensional Jet angularities and the two-dimensional primary lund plane (PLP). DNNs are employed to identify b Jets using these QCD-inspired observables. The DNNs are trained on a set of input features, which include Jet angularities and the PLP, in order to efficiently distinguish b Jets from light ones. The performance of the DNNs is evaluated by comparing their results with those of conventional track-based taggers, such as JetFitter, IP3D, and DL1 taggers. In this study, the results indicate that the DNN discriminants exhibit better performance than the IP3D tagger. The researchers in [33] discusses the application of DNNs to a wide range of physics problems, particularly in HEP. Specifically, DNNs have been successfully applied to tasks such as Jet tagging and event classification. The authors explore the use of a simple but effective preprocessing step that transforms observational quantities into a binary number with a fixed number of digits, representing the quantity or magnitude in different scales. This approach has been shown to significantly improve the performance of DNNs for specific tasks without complicating feature engineering, particularly in b-Jet tagging using daughter particles' momenta and vertex information.

Parton shower in **HEP** refers to the process where high-energy particles, such as quarks and gluons, emit further particles as they evolve, simulating the fragmentation and radiation patterns observed in particle collisions within particle accelerators, which is crucial for understanding particle interactions. Barnard et al., [15] advocate for **DNNs** as hadronic resonance taggers, trained on jet images generated from different generators. The **DNN** showed improved performance on test events generated by the default PYTHIA shower instead of using HERWIG and SHERPA generators, suggesting acquisition of PYTHIA-specific features. However, they noticed that biases may arise from generator approximations. They examine parton shower variations' impact on tagger performance using **LHC** data. Results show up to 50% differences in background rejection. They introduced the "zooming" method, enhancing performance between 10-20% across jet transverse momenta. Moving on, **generative adversarial network (GAN)** models have efficiently generated simulated data at lower costs but struggle with sparse data. The authors in [34] introduce a novel **DNN** model, called sparse autoregressive model (SARM), that learns data sparsity explicitly, yielding stable and interpretable results compared to **GANs**. In two case studies, the first, referred to as $D + D$, employs a discrete mixture model by discretizing pixel values using predetermined grid points, while the second, $D + C$, utilizes a discrete mixture model constructed with a truncated logistic distribution for pixel modeling. In two case studies, SARM outperforms **GANs** by 24-52% and 66-68% on images with high sparsity.

5.3. CNN-based

CNNs have revolutionized Jet image classification and prediction in particle physics. **CNNs** excel in image recognition by leveraging convolutional layers, weight sharing, and pooling to capture hierarchical features, enabling effective pattern recognition and classification [35, 36]. This enables precise particle identification using Jet images, improved event classification, and deeper insights into **HEP** experiments, advancing researchers' understanding of fundamental particles and interactions. For example, the study [37] demonstrates **CNN's** efficacy in predicting energy loss for quark and gluon Jets, yielding comparable results. It highlights distinctions post-quenching and employs deep learning for classification, emphasizing energy loss's impact on classification difficulty. The authors in [38] investigate the capability of **CNNs** in discriminating quark and gluon Jets, comparing their performance to traditionally designed physics observables. Similarly, in order to discriminate Quark-Gluon Jet, Lee et al. in their research [39], employed various pretrained **CNN** models, including VGG, ResNet, Inception-ResNet, DenseNet, Xception, Vanilla ConvNet, and Inception-ResNet, to classify Jet images for distinguishing quark and gluon hadron Jets. The study reveals that DenseNet outperforming larger, higher-structured networks. Despite marginal improvements over a traditional **BDT** classifier, stability in training can be enhanced using the RMSProp optimizer, an adaptive learning rate optimization algorithm.

In Figure 15, a CNN architecture is presented specifically designed for identifying quark and gluon Jets. Du et al. in their paper [40] addressed challenges in assessing Jet distribution modification in a hot **QCD** medium during heavy-ion collisions. It utilizes a **CNN** trained on a hybrid strong/weak coupling model, achieving good performance and emphasizing result interpretability. The study reveals discriminating power in the angular distribution of soft particles and explores the potential of **DL** for tomographic studies of Jet quenching. Oliveira et al. [41] applied a **CNN** directly to Jet images, showcasing its effectiveness as a powerful tool for identifying boosted hadronically decaying W bosons amid **QCD** multi-Jet processes. The researchers [1] employed **CNN** to analyze **LHC** proton-proton collision simulation data. Their **CNN** model, utilizing detector responses as images, distinguishes r-parity violating Super-symmetry (RPV SUSY) signal events from **QCD** multi-Jet background events. Achieving 1.85 times efficiency and 1.2 times expected significance over traditional methods. the authors showcased the model's scalability on HPC resources, reaching 1024 nodes.

In the realm of jet image classification, researchers proposed combining **CNN** with various other **DL** techniques. For instance, Farrell's paper [42], hybrid **DLs** revolutionize particle tracking. **LSTMs** excel in sequential data analysis, replacing Kalman filtering for hit assignment, while **CNNs** construct valuable detector data representations. Their fusion unveils a potent end-to-end model, with GPU training addressing traditional tracking algorithm scaling challenges. Similarly, significant progress resulted from integrating 1D **CNN** and **LSTM**, resulting in DeepJet NN model [9] for Jet identification. The architecture extract abstract features from three input collections—secondary vertices, charged particles (tracks), and neutral particles. The final jet flavor probabilities are determined by combining outputs with global Jet features in dense layers. This architecture was also applied to heavy flavour classification, with the model further adapted for quark-gluon tagging tasks [22].

5.4. Adversarial training-based

GANs in image processing enhance creativity and realism by generating new images through a dynamic interplay. The generator creates images, while the discriminator evaluates and refines them, enabling tasks like image-to-image translation, style transfer, and data augmentation with unparalleled versatility [36, 43]. **GANs** are powerful tools for Jet image classification in particle physics. They create realistic Jet images, enabling robust testing of classification algorithms. **GANs** enhance the accuracy of identifying particles and contribute to breakthroughs in **HEP** research. However, the authors in [44] employed another technique for adversarial training for physics object identification and decreased the effect of simulation-specific artifacts. They systematically distorted inputs that have been generated with **fast gradient sign method (FGSM)** adversarial attack technique, this latter altering model predictions using gradient information. The method showed how model performance and robustness are related. They explored the trade-off between performance on unperturbed and on distorted test samples, investigating ROC curves and AUC scores for the used discriminators. Similarly, in [45], the paper investigates the loss manifold of a Jet tagging algorithm concerning input features on nominal and adversarial samples. Discrepancies in flatness reveal differences in robustness and generalization. The study suggests refined training approaches through macro-scale loss manifold exploration for two features and devising attacks that maintain the gradient's directionality. This leverages acquired insights for enhanced object identification in particle physics.

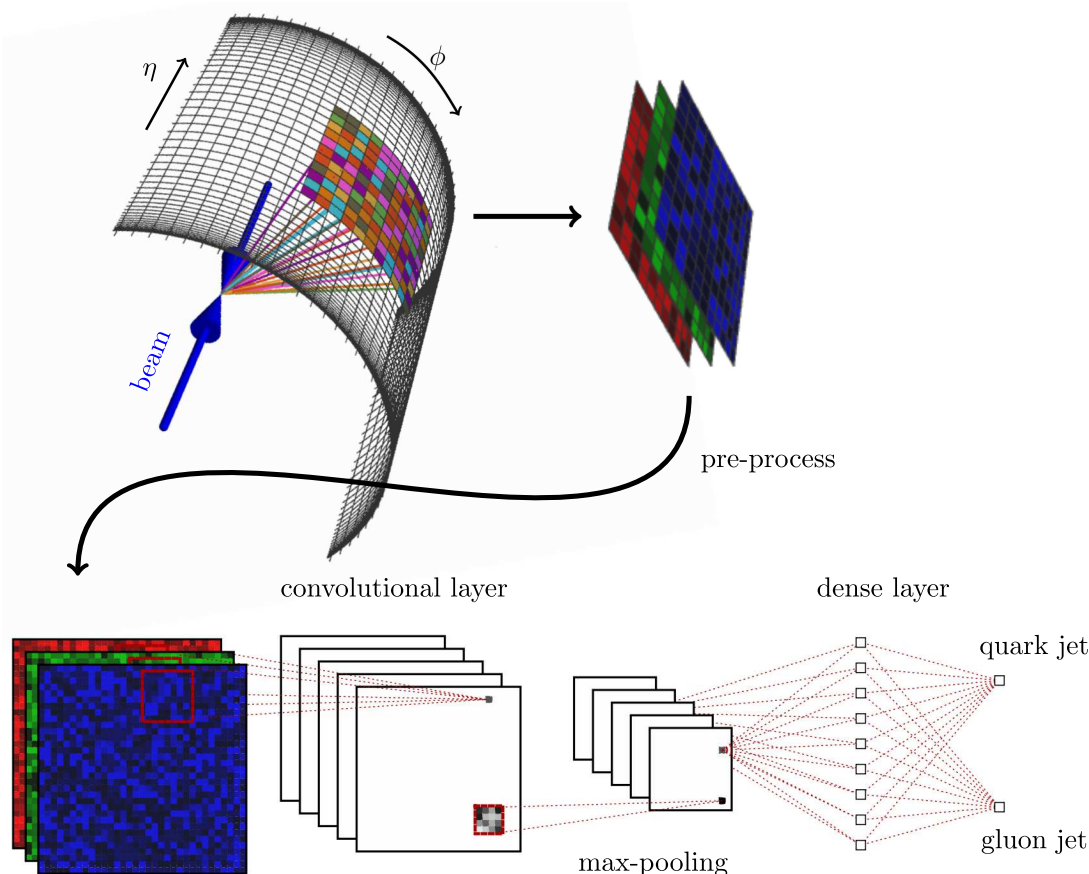


Figure 15: Example of CNN architecture with input Jet image, three convolutional layers, dense layer, and output layer are involved. In this context, **red** represents the transverse momenta of charged particles, **green** corresponds to the p_T of neutral particles, and **blue** signifies the charged particle multiplicity [38].

5.5. RNN-based

Various types of RNNs such as **bidirectional RNNs (BRNNs)**, **LSTM**, and **gated recurrent units (GRUs)** differ in architecture at the cell level within the RNN layer. **BRNNs** propagate information in both forward and backward directions, influencing predictions by surrounding words. **LSTM** tackles vanishing gradients with inner cells containing input, output, and forget gates, regulating information flow. **GRUs**-based networks address short-term memory issues with reset and update gates controlling information utilization akin to **LSTM** gates [35, 46]. **Recursive neural networks (RecNNs)**, are designed to operate on hierarchical or tree-structured data, where the relationships between elements are defined by a recursive structure. Instead of processing sequences sequentially with temporal dependencies, like RNNs, **RecNNs** recursively apply the same neural network operation to combine representations of child nodes to produce a representation of their parent node, traversing the hierarchical structure. In light of this, the authors in [47] investigate **RecNNs** for quark/gluon discrimination. Results indicate **RecNNs** outperform baseline, boosted decision tree, in gluon rejection rate by a few percent. Even with minimal input features such as p_T, η, ϕ , **RecNNs** yield promising results, suggesting tree structure contains essential discrimination information. Additionally, rough up or down quark jet discrimination is explored. In [46], a neural network was created specifically for Jet binary classifying. The network comprises two hidden layers employing recurrent cells, with a structure consisting of 25 **LSTM** cells and utilizing a tanh activation function at its core.

5.6. Other

MLP is an artificial neural network composed of multiple layers of nodes, including an input layer, one or more hidden layers, and an output layer. Each node in one layer is connected to every node in the subsequent layer. **MLP** can handle complex nonlinear relationships between input and output data, making them suitable for various tasks. **MLPs** are versatile, scalable, and can be trained using back-propagation, enabling them to learn from large datasets effectively and generalize well to unseen data. Kinematic parameters describe the motion of particles, including velocity, momentum ($p_{T,J}$) and trimmed jet momentum ($p_{T,J,trim}$), energy, jet mass m_J and jet mass trimmed $m_{J,trim}$, and angles of emission, commonly used in physics and engineering analyses. Chakraborty et al. in [48] employed both kinematics and spectral function, which typically refers to a function that describes the distribution of energy or momentum states of particles in a particular physical system, to feed **MLP** classifier as described in Figure 16. The authors aim is to trim/discard Jet that are unlikely to have originated from the process of interest (effects of background noise). This selective removal helps to improve the accuracy of measurements and analyses by focusing only on the most relevant particles within a jet.

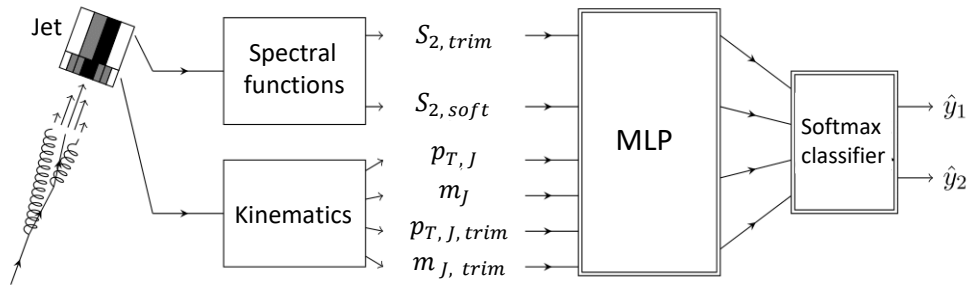


Figure 16: An example of classifier utilizing **MLP** trained using kinematic and spectrum variables for jet classification [48]. $S_{2,trim}$ and $S_{2,soft}$ correspond to hard and soft substructure information.

Table 6

Summary of the performance of certain deep learning frameworks proposed for **HEP**. Only the best performance is reported in the case of multiple tests.

Ref.	DLM	Dataset	Description	BP (%)	Limitations	PLA
[1]	CNN	QCD multi-jet	Classification of multi-Jet events using CNN at high energies of 13 TeV	AUC= 99.03	The proposed CNN model needs validation with additional datasets to ensure its generalizability.	No
[17]	SVM	Simulated	BIP features invariant under boosts for improved Jet tagging	Acc= 92.7	Performance could be enhanced through comprehensive hyperparameter tuning.	Yes ¹²
[25]	DNN	Simulated	Sequence of jet components arranged in a specific order for training inputs.	Acc= 50	Could be enhanced by employing the LSTM method to efficiently classify Jet from background.	No
[30]	DNN	Simulated ¹³	DNNs for categorizing Jet substructure in HEP	AUC= 95.3	The accuracy of the DNN models is limited by the accuracy of the simulation models used to generate the training data.	No
[31]	DNN	Higgs	Clarifying HEP event classification with SHAP	Acc= 66	SHAP may not comprehensively capture feature interactions or explain model behavior in all cases. It could demand substantial computational resources for large datasets or intricate models.	Yes ¹⁴
[32]	DNN	ATLAS	Detection of b Jets utilizing QCD -inspired measurements	AUC= 67	The DNN performed slightly less effectively than the JetFitter algorithm.	No
[34]	DNN	Pythia Jet images	Creating images with low pixel density in particle physics for two cases $D + D$ and $D + C$.	AUC= 86.9, AUC= 84.1	Slower than the non-autoregressive model LAGAN. $D + D$ performed better than $D + C$ for both Pythia and Monte Carlo images.	Yes ¹⁵
[37]	CNN	Simulated	CNN for predicting quark and gluon Jets	Acc= 75.9	The higher the energy loss, the more challenging the task of classifying the Jets becomes.	No
[47]	RecNN	Simulated	Enhance Quark/gluon classification	AUC= 86.37	Event-level analysis is not performed.	Yes ¹⁶
[49]	CNN and AE	Daya Bay	Classification for different event types, including IBD prompt, IBD delay, Muon, Flasher, and other	Acc= 99.9 (Muon)	SVM and KNN exhibit inferior performance compared to CNN in identifying event types. Moreover, semi-supervised techniques have not been examined.	No
[50]	CNN	Simulated	Employing a quantum CNN to categorize events in HEP .	Acc= 97.5	Quantum CNN showed a lower performance than CNN when it comes to a binary classification of Muon and Electron . Besides, CNN showed low performance when classifying Muon and Pion compared to quantum CNN .	No
[51]	ML	ATLAS	Predict if the LHC trials have dismissed a new physics model	Acc= 93.8	Enhancing reliability can be achieved by requiring a minimum confidence level for the prediction.	Yes ¹⁷
[52]	ANN	Simulated	Identifying boosted top quarks using pattern recognition through an ANN in HEP experiments.	Eff= 60	It has 4% mis-tag rate. It exclusively utilizes hadronic calorimeter (HCAL) data, though additional data, like sub-jet b-tags, are crucial for top tagging.	No
[53]	DNN	Real data	Enhancing jet reconstruction at CMS through deep learning	FPR= 65	The computational costs, when employing the proposed model, have not been verified.	No

Abbreviations: Deep learning model (DLM); Best performance (BP); Project link availability (PLA).

6. Applications of AI-based Jet image

Jet images processed through **ML** and **DL** techniques hold vast potential across various applications within the **HEP** domain, some of them are already described in [2]. This section presents a comprehensive overview of cutting-edge work in this area, categorized into several key domains: Jet parameter scanning, event classification, Jet tagging, multi-Jet classification, energy estimation, and beyond. The taxonomy of AI-based jet image applications is visualized in Figure 17, illustrating their scope

¹²<https://zenodo.org/records/7271316>

¹³<https://www.igb.uci.edu/~pfbaldi/physics/>

¹⁴https://github.com/rpezoa/hep_shap/

¹⁵<http://mlphysics.ics.uci.edu/>

¹⁶<https://github.com/gloupe/recnn>

¹⁷<http://susyai.hepforge.org>

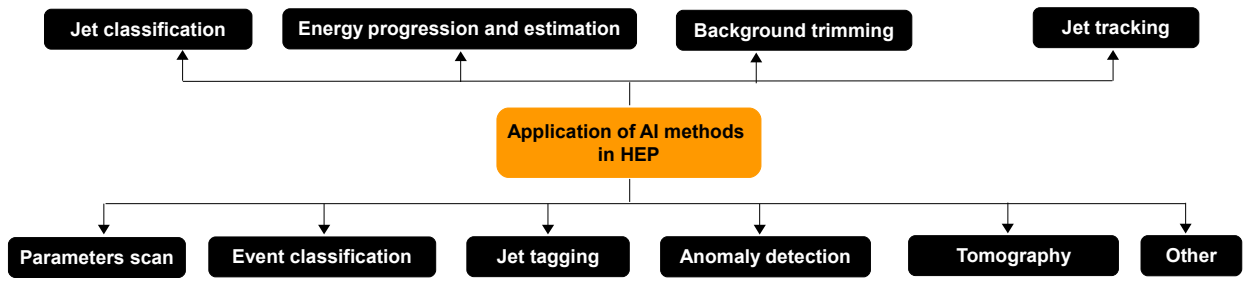


Figure 17: Taxonomy of AI-based HEP applications using Jet images.

and relationships. The section thoroughly reviews some applications conducted by researchers, while suggesting future directions for those not yet explored. Additionally, Table 6 provides a concise summary of performance metrics, limitations, online project availability, and results obtained across these applications, offering valuable insights into their efficacy and applicability.

[54]

6.1. Parameters scan

The utilization of a **ML** and **DL** models enables the comprehension and estimation of the correlation between the parameter space of the new physics model and the experimental physical observables. This facilitates the efficient constraint of the parameter space of the new physics model [2]. Given the sensitivity of the ATLAS experiment to exploring the parameters and event counts in a new physics, significant computing power is required to deduce the surviving regions of the parameter space of **constrained minimal super-symmetric standard model (CMSSM)** using Bayesian posterior probability and likelihood function ratio test. To mitigate computational demands, the study [55] utilizes a **MLP** as a regressor to learn the mapping from **CMSSM** model parameters θ to weak-scale super-symmetric particle masses m . The output of the SoftSusy physical package serves as the target output value of the neural network. Approximately 4000 sample points in the parameter space form the training set to train the regressor. With a given set of **CMSSM** parameters, this **MLP** model rapidly predicts the corresponding super-symmetric particle mass spectrum. This approach significantly accelerates the process compared to traditional methods. To identify the parameters of a new physics model, [56], a **MLP** was trained using 84 physical observables from the 14 TeV **LHC** as inputs, with the parameters of a super-symmetric model as the desired outputs. The study revealed that with a collider luminosity of $10 fb^{-1}$, the **CMSSM** model's parameters M_0 and $M_{1/2}$ could be reliably determined with just a 1% margin of error. With a collider luminosity of $500 fb^{-1}$, additional model parameters such as $\tan \beta$ and A_0 could also be accurately estimated. In contrast, the conventional approach of minimizing χ^2 yielded comparatively inferior results. Generating collider event samples at the **LHC** through Monte Carlo simulation can be a time-intensive process. While a rapid detector simulation typically requires only a few minutes, a comprehensive simulation using the GEANT4 framework, as employed by experimental groups like ATLAS and CMS, may necessitate several days. To address this, parallel full detector simulations are conducted using four parameters, namely common scalar mass (m_0), the universal gaugino mass ($m_{1/2}$), the trilinear coupling term (A_0), and the ratio of the vacuum expectation values ($\tan \beta$) [57]. Two **ML** models, namely the **MLP** and **SVM**, were employed to learn the correlation between the number of signal events and the **CMSSM** parameters. Results showed that the accuracy of predicting the likelihood function could reach several percent with just 2000 training samples.

6.2. Jet classification and tagging

Despite treating Jets as images in the calorimeter and exploiting the benefits of **DNNs** in image classification for improved Jet substructure detection, these approaches encounter hurdles. Challenges such as Jet image sparsity and potential precision loss arise from constructing Jet images through pixelation or creating advanced Jet features. In this study [25], a sequential method is employed, utilizing an ordered sequence of jet constituents as inputs for training. Unlike many prior methods, this approach avoids information loss during pixelization or high-level feature computation. The Jet classification technique achieves a considerable background rejection efficiency operating point for reconstructed jets with transverse momentum ranging from 600 to 2500 GeV. Moreover, it remains unaffected by multiple proton-proton interactions at levels anticipated during Run 2 of the **LHC**.

Particles generated in a collider with significant center-of-mass energy typically exhibit high velocity. As a result, their decay products tend to align closely, leading to overlapping jets. It is crucial in collider data analysis to discern whether a jet originates from a solitary light particle or from the decay of a heavier particle. Traditional approaches rely on manually crafted distribution features based on energy deposition in calorimeter cells. However, due to the intricate nature of the data, **ML** techniques have proven more efficient than human efforts for this task [58]. In [59], the Jet image concept treats the detector as a camera, capturing Jet energy distribution in calorimeters as a digital image. This enables Jet tagging as a pattern recognition task, utilizing machine learning, like Fisher classification, to differentiate between hadronic W boson decay and Jets from quarks or gluons. Monte Carlo simulation shows superior discrimination compared to traditional methods, offering insights into Jet structure. In [38], **CNNs** improve tagging by treating Jet energy distribution as an image, using channels for features like particle momentum and count. Results show **CNNs** can surpass traditional methods, providing reliable insights from collider simulation data despite variations in event generators. However, **CNNs** demonstrate a lack of sensitivity to quark/gluon Jets from different generators, akin to conventional Jet measurements. Moving on, in [60], Jet tagging is performed using **RNN**, leveraging the similarity between Jet

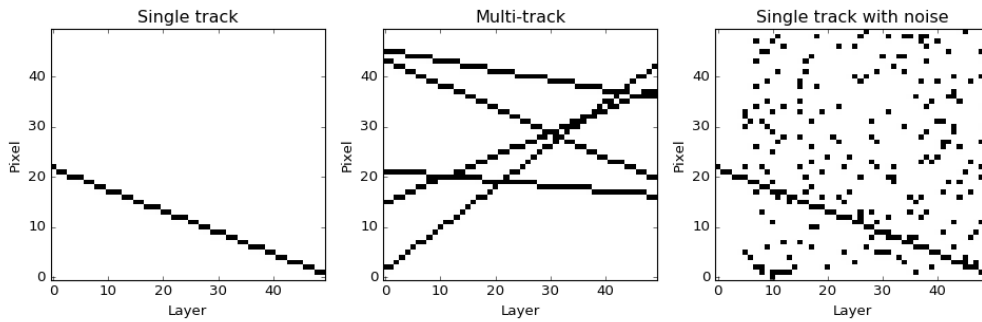


Figure 18: A toy dataset with adjustable dimensions, straight line representations for tracks, and the option to include uniform noise hits, all on a smaller scale.

clustering and natural language structure. Final-state particle four-momenta are treated as language words, and Jet clustering as grammatical analysis. **RNN** efficiently processes the tree-like Jet structures, enabling direct use of particle data regardless of count. This method yields higher data utilization efficiency and prediction accuracy than Jet image-based **ML**, extending to event classification. In [47], **RNNs** distinguish quark and gluon Jets, showing higher gluon suppression. Factors affecting **RNN** performance are explored, with preliminary quark tagging results. Numerous explorations for phenomena beyond the **SM** at the **LHC** depend on top tagging techniques that distinguish between boosted hadronic top quarks and the more prevalent jets that originate from light quarks and gluons. The **HCAL** essentially captures a "digital image" of each jet, where the pixel brightness represents the energy deposited in **HCAL** cells. Therefore, top tagging is essentially a matter of recognizing patterns. The work in [52] propose a novel top tagging algorithm based on an **ANN**, a popular pattern recognition approach. The **ANN** is developed using a substantial dataset of boosted tops along with light quark/gluon jets and is subsequently evaluated on separate datasets. In Monte Carlo simulations, particularly within the 1100-1200 GeV range, the **ANN**-based tagger demonstrates outstanding efficacy.

Efficient **HEP** data analysis is imperative with the surge in data from modern particle detectors. However, detectors have limited access to the substructure of jets, especially those distant from the center-of-mass frame. To address this, the authors [17] integrate **BIP** features with standard classification methods, significantly improving Jet tagging efficiency. Notably, supervised methods like **MLP**, **XGBoost**, **LogReg**, **SVM**, and unsupervised approaches like **Gaussian mixture model (GMM)** and **KNN** achieve exceptional performance with **uniform manifold approximation and projection (UMAP)** dimensionality reduction technique, surpassing contemporary **DL** systems while reducing training and evaluation times significantly. In [53], the authors introduce a novel network architecture designed for jet tagging in experiments conducted at the **LHC**. **DeepCSV**, currently endorsed by **CMS** and employing a **DNN**, has significantly improved tagging performance, as validated using real collision data. It surpasses other tagging methods, particularly at high transverse momenta, with nearly an order of magnitude reduction in **FPRs** using standard threshold definitions.

Multi-jet classification is a key task in particle physics aimed at distinguishing between events with varying numbers of jets. Using **ML** techniques, such as **DNNs**, researchers develop classification models to accurately identify these events. Achieving high classification accuracy is crucial for understanding fundamental particle interactions and discovering new physics phenomena in experiments like those conducted at the **LHC**. The work in [1] present an application of scalable **DL** to analyze simulation data from proton-proton collisions at 13 TeV in the **LHC**. The researchers developed a **CNN** model which utilizes detector responses as two-dimensional images reflecting the geometry of the **CMS** detector. The model discriminates between signal events of R-parity violating super-symmetry and background events with multiple jets resulting from inelastic **QCD** scattering (**QCD** multi-jets). With the **CNN** model, they achieved 1.85 times higher efficiency and 1.2 times higher expected significance compared to the traditional cut-based method. They demonstrated the scalability of the model at a large scale using **high-Performance computing (HPC)** resources with up to 1024 nodes. The authors in [48] proposing an interpretable network for multi-jet classification using the jet spectrum, termed **S2(R)**, derived from a Taylor series of an arbitrary jet **MLP** classifier function. The network's intermediate feature is an infrared and collinear safe variables, named **C-correlator**, estimating the importance of **S2(R)** deposits at angular scales. It offers comparable performance to **CNNs** with simpler architecture and fewer inputs.

6.3. Jet tracking

Jet tracking involves reconstructing the trajectories and properties of particles within jets, formed when quarks and gluons fragment. Accurate tracking is vital for particle physics analyses, aiding in discoveries, **SM** measurements, and searches for new phenomena. Advanced algorithms, including pattern recognition and **ML**, are employed for precise tracking in modern detectors. In this research paper [42], the authors present early attempts at applying **ML** techniques to address particle tracking challenges. This area remains largely unexplored, and they have just scratched the surface. Nonetheless, certain **DL** methods show promise. **LSTMs** were found to be effective in solving the hit assignment problem in both 2D and 3D scenarios using a sequence of detector layer measurements, potentially offering an alternative to the combinatorial Kalman Filter. **CNNs** demonstrated the ability to construct representations of detector data from the ground up, aiding in hit assignment and parameter/uncertainty estimation. Through the combination of **LSTM** and **CNN**, the authors showcased a potentially powerful end-to-end model capable of identifying a variable number of tracks within detector images. Figure 18 displays sample 2D data generated with various types of tracks, including single-track, multi-track, and single-track with uniform noise.

6.4. Jet image generation

In order to study new physics phenomena at the LHC, it is necessary to simulate Monte Carlo events for both new physics signals and backgrounds. This simulation helps predict the experimental data expected from collider experiments. However, generating the large number of simulated events required for data analysis is time-consuming and computationally intensive using existing algorithms. Additionally, accurately simulating how energetic particles interact with detector materials can be a time-consuming process. In [61], researchers proposed using GANs to build LAGAN framework, that is trained to generate authentic radiation distributions from simulated collisions involving high-energy particles. The authors found that the generated Jet images exhibited a wide range of pixel brightness levels and accurately reproduced low-dimensional physical observables such as reconstructed Jet mass and n-subjettiness. However, the study also acknowledges the limitations of this method and presents an empirical validation of the image quality. With further improvement, this approach could lead to faster simulation of HEPs events. Physicists at the LHC use complex simulations to predict experimental outcomes. Generating vast amounts of simulated data is costly, but crucial for technique development. Challenges include accurately modeling detectors and particle interactions. In [62], researchers proposed a GAN-nased model for fast, accurate simulation of electromagnetic calorimeters. Despite ongoing precision challenges, our solution offers significant speed-ups, up to 100,000 \times , promising savings in computing resources and advancing physics research at the LHC and beyond.

7. Future direction and outlook

The future of ML and DL in HEP, particularly in jet analysis, is poised for transformative advancements. As researchers delve deeper into the petabyte-scale datasets generated by experiments like those at the LHC and QCD, the role of DL becomes increasingly vital. The potential implications of QML-baset Jet research for future particle physics experiments are significant. By demonstrating the effectiveness of QML for jet classification in section 5.1, this opens up new possibilities for improving the performance of particle physics experiments. Researchers could apply the suggested QML-based approaches to jet images to other HEP problems, such as signal versus background separation, anomaly detection, and particle track reconstruction. Furthermore, QML-based research on jet images could pave the way for the development of new quantum algorithms and hardware that could be used to solve complex problems in particle physics and other fields.

There are multiple other compelling aspects and potential extensions that warrant further exploration, which are outlined here. For examples, for *event-level analysis*, a jet, in essence, cannot be entirely separated from an event's remaining parts, yet "pure" jets can be achieved through grooming techniques. The utility of color connections is notable in various scenarios. The exploration into how to effectively demonstrate these effects is important, as there is potential in enhancing event-level analysis. The RNN approach, particularly RecNN, is easily adaptable for event-level analysis due to its natural fit into larger hierarchical structures. Previous studies have examined event analysis focusing solely on jets, utilizing simple RNN chains to reconstruct events from jets. When considering event-level implementation, structuring the entire event poses a significant challenge. Viewing each event as a structured data tree, where the entire event's information is encapsulated in the nodes' properties and their interconnections, is vital. Therefore, accurately representing each element and its connections within the event is crucial for developing neural network architectures. For *Jet unsupervised learning*, within the DNN framework, adjusting jet clustering could potentially enhance performance. Treating jet finding as a minimization problem presents an intriguing perspective, making it appealing to incorporate jet finding processes directly into event-level analysis. Another example, for *new physics phenomena* often display distinctive patterns related to their particle spectrum and decay modes. For instance, supersymmetry (SUSY) events typically generate a high number of final states, presenting a more complex hierarchical structure, and may include several soft leptons in electroweakino searches. Investigating whether DNNs can more effectively accommodate such topologies is also a worthwhile endeavor [47]. Moreover, distinguishing between quark-initiated and gluon-initiated Jets is crucial in collider experiments like the LHC. Discriminating between these Jets is challenging due to complex correlations in radiation patterns and non-perturbative effects like hadronization. AI methods, such as deep generative models, offer promising solutions to address this challenge [38]. Moving forward, there is a notable scarcity of published research on the application of auto-encoder (AE) for jet image processing, highlighting an opportunity for researchers to explore this field further. The potential for AE to significantly improve the separation of jet images from background noise presents a promising area of study. By focusing on this niche, researchers can contribute to advancing our understanding and methodologies in particle physics, potentially leading to more accurate and efficient analysis techniques.

The complexity and volume of the data necessitate sophisticated analytical techniques that DL models, especially those based on CNNs and GNNs, are well-equipped to handle. These models excel in identifying intricate patterns and correlations within the data, making them invaluable for tasks such as jet tagging, particle tracking, and event classification. Furthermore, the scalability of DL models needs to be addressed to handle the increasing data rates from next-generation detectors and accelerators. Efficient training algorithms and model compression techniques will be essential for deploying these models in real-time analysis frameworks, enabling faster decision-making processes for data acquisition and retention. The future of DL in *jet energy progression and estimation* promises enhanced precision and efficiency. Innovations will likely focus on developing more sophisticated neural network models that can accurately predict jet energies in complex environments. Emphasis on real-time data analysis capabilities and integration with experimental workflows will be crucial, driving advancements in detecting and interpreting high-energy particle collisions more effectively and swiftly. The future of DL-based jet *anomaly detection* in HEP lies in advancing unsupervised learning techniques to uncover new physics signals hidden in complex data. Innovations in model interpretability and real-time processing will enhance detection capabilities. Cross-disciplinary collaboration will drive these advancements, leading to breakthroughs in identifying rare phenomena and expanding our understanding of the fundamental constituents of the universe. Others applications such as *flavor tagging*, *pileup mitigation*, and the *reconstruction of decay chains*. These DL-based Jet images

can help in distinguishing between different types of particles based on their energy deposition patterns, aiding in the precise determination of particle origins and decay pathways. Additionally, they can be used for enhancing signal-to-noise ratios in complex collision environments, improving the accuracy of particle trajectory tracking, and in the analysis of jet substructure to identify specific decay processes, contributing to a deeper understanding of the underlying physics in high-energy collisions. The application of DL-based HEP jet images for *tomography* is promising. This approach has the potential to revolutionize how we visualize and analyze subatomic particles, offering unprecedented precision and insight. By leveraging DL techniques, researchers can improve the accuracy of tomographic reconstructions, enhancing our understanding of particle interactions and the fundamental structure of matter.

Transfer learning (TL) detailed in [63–65], is poised to revolutionize Jet HEP applications by leveraging pre-trained models from vast datasets to enhance performance on specific tasks with limited data. This approach can significantly reduce computational costs and training times, making it ideal for adapting models to new experiments or rare phenomena. As HEP experiments generate increasingly complex data, the ability to apply knowledge from one context to another will be invaluable for improving event classification, anomaly detection, and signal processing. Looking ahead, transfer learning will be crucial for efficiently extracting insights from new particle interactions and advancing our understanding of fundamental physics. Exploring advanced CNN architectures as source of prior knowledge like AlexNet, Fast-R-CNN, VGG, ResNet, GoogLeNet could offer potential improvements to target model that conduct many AI-based Jet tasks [24]. Generalizing the top tagger to classify other boosted objects, such as W/Z bosons, Higgs bosons, and BSM particles, is straightforward and extending it to partially-merged and fully resolved tops could enhance background rejection.

Reinforcement learning (RL), with all its variants [66], in HEP jet applications is set to open novel pathways for optimizing experimental setups and data analysis strategies. By leveraging RL's ability to learn optimal policies through interaction with an environment, future HEP experiments could see enhanced automation in event selection, detector alignment, and real-time data processing. The adaptability of RL models to dynamic systems makes them particularly suited for managing the complexities of particle collision events. As the technology matures, integrating RL into HEP could lead to significant advancements in experiment efficiency, discovery potential, and the ability to navigate vast datasets to uncover new physics phenomena. Additionally, **federated learning (FL)**-based computer vision [67] presents a promising frontier for Jet images applications, offering a pathway to harness collaborative model training while preserving data privacy and security. By distributing the learning process across multiple nodes, each holding its own subset of data, FL enables a collective improvement of models without direct data sharing. This approach is particularly suited for HEP collaborations spread across global institutions, where data locality and privacy concerns can limit traditional centralized training methods. Advancements in FL could lead to more robust, accurate models, enhancing our understanding of complex particle physics phenomena through cooperative, privacy-preserving analysis between different LHCs.

8. Conclusion

Given the comprehensive assessment of ML and DL applications within the realm of HEP presented in this survey, it is evident that these techniques have significantly impacted various aspects of HEP experimentation and phenomenological studies. Through a detailed exploration of diverse DL approaches, including their application to HEP image classification, Jet particle analysis, and other pertinent areas, this paper has highlighted the potential of ML and DL techniques to enhance our understanding of particle physics phenomena. The analysis undertaken throughout this survey underscores the importance of leveraging AI models tailored to HEP images, as well as the significance of state-of-the-art ML and DL techniques in advancing HEP inquiries. Specifically, the review has elucidated the implications of these techniques for tasks such as Jet tagging, Jet tracking, and particle classification, shedding light on their capabilities and limitations in addressing key challenges within the field. As we reflect on the current status of HEP grounded in DL methodologies, it becomes evident that while significant progress has been made, there remain inherent challenges that must be addressed to fully harness the potential of these approaches. These challenges include issues related to data quality, model interpretability, and generalization to diverse experimental conditions. Nonetheless, the survey also identifies promising avenues for future research endeavors, such as the development of novel DL architectures tailored to HEP data and the integration of domain-specific knowledge to enhance the performance of learning models. By addressing the challenges and leveraging the opportunities highlighted in this survey, researchers can continue to push the boundaries of HEP experimentation and pave the way for groundbreaking discoveries in particle physics using AI techniques.

References

- [1] J. Kim, C.-S. Moon, H. Nam, J. Goh, D. Bae, C. Yoo, S. Kim, T. Kim, H. Yoo, S. Hwang, et al., Multi-jet event classification with convolutional neural network at large scale, in: *Journal of Physics: Conference Series*, Vol. 2438, IOP Publishing, 2023, p. 012103.
- [2] M. Abdughani, J. Ren, L. Wu, J.-M. Yang, J. Zhao, Supervised deep learning in high energy phenomenology: a mini review, *Communications in Theoretical Physics* 71 (8) (2019) 955.
- [3] W. Guan, G. Perdue, A. Pesah, M. Schuld, K. Terashi, S. Vallecorsa, J.-R. Vlimant, Quantum machine learning in high energy physics, *Machine Learning: Science and Technology* 2 (1) (2021) 011003.
- [4] A. Stakia, T. Dorigo, G. Banelli, D. Bortoletto, A. Casa, P. de Castro, C. Delaere, J. Donini, L. Finos, M. Gallinaro, et al., Advances in multi-variate analysis methods for new physics searches at the large hadron collider, *Reviews in Physics* 7 (2021) 100063.
- [5] E. G. Blackman, S. V. Lebedev, Persistent mysteries of jet engines, formation, propagation, and particle acceleration: Have they been addressed experimentally?, *New Astronomy Reviews* (2022) 101661.
- [6] S. Banerjee, Fifty years of experimental high energy physics, *Indian Journal of Physics* (2023) 1–17.
- [7] H. Lv, D. Wang, L. Wu, Deep learning jet images as a probe of light higgsino dark matter at the lhc, *Physical Review D* 106 (5) (2022) 055008.

- [8] A. Gianelle, P. Koppenburg, D. Lucchesi, D. Nicotra, E. Rodrigues, L. Sestini, J. de Vries, D. Zuliani, Quantum machine learning for b-jet charge identification, *Journal of High Energy Physics* 2022 (8) (2022) 1–24.
- [9] A. Novak, Sissa: Heavy flavour jet identification with the cms experiment in run 2, *PoS* (2020) 146.
- [10] A. Blance, M. Spannowsky, Quantum machine learning for particle physics using a variational quantum classifier, *Journal of High Energy Physics* 2021 (2021) 1–20.
- [11] R. Cheng, Quantum geometric tensor (fubini-study metric) in simple quantum system: A pedagogical introduction, arXiv preprint arXiv:1012.1337 (2010).
- [12] A. Di Luca, M. Cristoforetti, R. Iuppa, D. Mascione, Automated feature selection procedure for particle jet classification, *Nuclear Physics B* 990 (2023) 116182.
- [13] S. Gong, Q. Meng, J. Zhang, H. Qu, C. Li, S. Qian, W. Du, Z.-M. Ma, T.-Y. Liu, An efficient lorentz equivariant graph neural network for jet tagging, *Journal of High Energy Physics* 2022 (7) (2022) 1–22.
- [14] M. Cacciari, G. P. Salam, G. Soyez, The anti-kt jet clustering algorithm, *Journal of High Energy Physics* 2008 (04) (2008) 063.
- [15] J. Barnard, E. N. Dawe, M. J. Dolan, N. Rajcic, Parton shower uncertainties in jet substructure analyses with deep neural networks, *Physical Review D* 95 (1) (2017) 014018.
- [16] G. C. Strong, On the impact of selected modern deep-learning techniques to the performance and celerity of classification models in an experimental high-energy physics use case, *Machine Learning: Science and Technology* 1 (4) (2020) 045006.
- [17] J. M. Munoz, I. Batatia, C. Ortner, Boost invariant polynomials for efficient jet tagging, *Machine Learning: Science and Technology* 3 (4) (2022) 04LT05.
- [18] H. Qu, C. Li, S. Qian, Particle transformer for jet tagging, in: *International Conference on Machine Learning*, PMLR, 2022, pp. 18281–18292.
- [19] V. G. Satorras, E. Hoogeboom, M. Welling, E (n) equivariant graph neural networks, in: *International conference on machine learning*, PMLR, 2021, pp. 9323–9332.
- [20] H. Qu, L. Gouskos, Jet tagging via particle clouds, *Physical Review D* 101 (5) (2020) 056019.
- [21] A. Bogatskiy, B. Anderson, J. Offermann, M. Roussi, D. Miller, R. Kondor, Lorentz group equivariant neural network for particle physics, in: *International Conference on Machine Learning*, PMLR, 2020, pp. 992–1002.
- [22] E. Bols, J. Kieseler, M. Verzetti, M. Stoye, A. Stakia, Jet flavour classification using deepjet, *Journal of Instrumentation* 15 (12) (2020) P12012.
- [23] P. T. Komiske, E. M. Metodiev, J. Thaler, Energy flow networks: deep sets for particle jets, *Journal of High Energy Physics* 2019 (1) (2019) 1–46.
- [24] S. Macaluso, D. Shih, Pulling out all the tops with computer vision and deep learning, *Journal of High Energy Physics* 2018 (10) (2018) 1–27.
- [25] J. Pearkes, W. Fedorko, A. Lister, C. Gay, Jet constituents for deep neural network based top quark tagging, arXiv preprint arXiv:1704.02124 (2017).
- [26] A. Blance, M. Spannowsky, Unsupervised event classification with graphs on classical and photonic quantum computers, *Journal of High Energy Physics* 2021 (8) (2021) 1–26.
- [27] L. Funcke, T. Hartung, B. Heinemann, K. Jansen, A. Kropf, S. Kühn, F. Meloni, D. Spataro, C. Tüysüz, Y. C. Yap, Studying quantum algorithms for particle track reconstruction in the luxe experiment, in: *Journal of Physics: Conference Series*, Vol. 2438, IOP Publishing, 2023, p. 012127.
- [28] K. K. Sharma, Quantum machine learning and its supremacy in high energy physics, *Modern Physics Letters A* 36 (02) (2021) 2030024.
- [29] S. L. Wu, S. Sun, W. Guan, C. Zhou, J. Chan, C. L. Cheng, T. Pham, Y. Qian, A. Z. Wang, R. Zhang, et al., Application of quantum machine learning using the quantum kernel algorithm on high energy physics analysis at the lhc, *Physical Review Research* 3 (3) (2021) 033221.
- [30] P. Baldi, K. Bauer, C. Eng, P. Sadowski, D. Whiteson, Jet substructure classification in high-energy physics with deep neural networks, *Physical Review D* 93 (9) (2016) 094034.
- [31] R. Pezoa, L. Salinas, C. Torres, Explainability of high energy physics events classification using shap, in: *Journal of Physics: Conference Series*, Vol. 2438, IOP Publishing, 2023, p. 012082.
- [32] O. Fedkevych, C. K. Khosa, S. Marzani, F. Sforza, Identification of b jets using qcd-inspired observables, *Physical Review D* 107 (3) (2023) 034032.
- [33] J. S. H. Lee, I. Park, S. Park, Multi-scale distributed representation for deep learning and its application to b-jet tagging, *Journal of the Korean Physical Society* 72 (2018) 1292–1300.
- [34] Y. Lu, J. Collado, D. Whiteson, P. Baldi, Sparse autoregressive models for scalable generation of sparse images in particle physics, *Physical Review D* 103 (3) (2021) 036012.
- [35] H. Kheddar, M. Hemis, Y. Himeur, D. Megías, A. Amira, Deep learning for steganalysis of diverse data types: A review of methods, taxonomy, challenges and future directions, *Neurocomputing* (2024) 127528doi:<https://doi.org/10.1016/j.neucom.2024.127528>.
- [36] Y. Habchi, Y. Himeur, H. Kheddar, A. Boukabou, S. Atalla, A. Chouchane, A. Ouamane, W. Mansoor, Ai in thyroid cancer diagnosis: Techniques, trends, and future directions, *Systems* 11 (10) (2023) 519.
- [37] Y.-L. Du, D. Pablos, K. Tywoniuk, Classification of quark and gluon jets in hot qcd medium with deep learning, arXiv preprint arXiv:2112.00681 (2021).
- [38] P. T. Komiske, E. M. Metodiev, M. D. Schwartz, Deep learning in color: towards automated quark/gluon jet discrimination, *Journal of High Energy Physics* 2017 (1) (2017) 1–23.
- [39] J. S. H. Lee, I. Park, I. J. Watson, S. Yang, Quark-gluon jet discrimination using convolutional neural networks, *Journal of the Korean Physical Society* 74 (2019) 219–223.
- [40] Y. Du, D. Pablos, K. Tywoniuk, Deep learning jet modifications in heavy-ion collisions (2020), arXiv preprint arXiv:2012.07797.
- [41] L. de Oliveira, M. Kagan, L. Mackey, B. Nachman, A. Schwartzman, Jet-images—deep learning edition, *Journal of High Energy Physics* 2016 (7) (2016) 1–32.
- [42] S. Farrell, D. Anderson, P. Calafiura, G. Cerati, L. Gray, J. Kowalkowski, M. Mudigonda, P. Spentzouris, M. Spiropoulou, A. Tsaris, et al., The hep. trkx project: deep neural networks for hl-lhc online and offline tracking, in: *EPJ Web of Conferences*, Vol. 150, EDP Sciences, 2017, p. 00003.
- [43] F. Rehm, S. Vallecorsa, V. Saletore, H. Pabst, A. Chaibi, V. Codreanu, K. Borrás, D. Krücker, Reduced precision strategies for deep learning: a high energy physics generative adversarial network use case, arXiv preprint arXiv:2103.10142 (2021).
- [44] A. Stein, X. Coubez, S. Mondal, A. Novak, A. Schmidt, Improving robustness of jet tagging algorithms with adversarial training, *Computing and Software for Big Science* 6 (1) (2022) 15.
- [45] A. Stein, Improving robustness of jet tagging algorithms with adversarial training: exploring the loss surface, arXiv preprint arXiv:2303.14511 (2023).
- [46] S. Auricchio, F. Crotto, A. Giannini, Vbf event classification with recurrent neural networks at atlas’s lhc experiment, *Applied Sciences* 13 (5) (2023) 3282.
- [47] T. Cheng, Recursive neural networks in quark/gluon tagging, *Computing and Software for Big Science* 2 (1) (2018) 3.
- [48] A. Chakraborty, S. H. Lim, M. M. Nojiri, Interpretable deep learning for two-prong jet classification with jet spectra, *Journal of High Energy Physics* 2019 (7) (2019) 1–36.
- [49] E. Racah, S. Ko, P. Sadowski, W. Bhimji, C. Tull, S.-Y. Oh, Exploring raw hep data using deep neural networks (2016).
- [50] S. Y.-C. Chen, T.-C. Wei, C. Zhang, H. Yu, S. Yoo, Quantum convolutional neural networks for high energy physics data analysis, *Physical Review Research* 4 (1) (2022) 013231.
- [51] S. Caron, J. S. Kim, K. Rolbiecki, R. R. de Austri, B. Stienen, The bsm-ai project: Susy-ai—generalizing lhc limits on supersymmetry with machine learning, *The European Physical Journal C* 77 (2017) 1–25.
- [52] L. G. Almeida, M. Backović, M. Cliche, S. J. Lee, M. Perelstein, Playing tag with ann: boosted top identification with pattern recognition, *Journal of High Energy Physics* 2015 (7) (2015) 1–21.
- [53] M. Stoye, C. collaboration, et al., Deep learning in jet reconstruction at cms, in: *Journal of Physics: Conference Series*, Vol. 1085, IOP Publishing, 2018, p. 042029.

- [54] M. Kagan, Image-based jet analysis, in: *Artificial Intelligence For High Energy Physics*, World Scientific, 2022, pp. 439–496.
- [55] M. Bridges, K. Cranmer, F. Feroz, M. Hobson, R. Ruiz de Austri, R. Trotta, A coverage study of the cmsm based on atlas sensitivity using fast neural networks techniques, *Journal of High Energy Physics* 2011 (3) (2011) 1–23.
- [56] N. Bornhauser, M. Drees, Determination of the cmsm parameters using neural networks, *Physical review d* 88 (7) (2013) 075016.
- [57] A. Buckley, A. Shilton, M. White, Fast supersymmetry phenomenology at the large hadron collider using machine learning techniques, *Computer Physics Communications* 183 (4) (2012) 960–970.
- [58] B. Bhattacharjee, S. Mukherjee, R. Sengupta, Study of energy deposition patterns in hadron calorimeter for prompt and displaced jets using convolutional neural network, *Journal of High Energy Physics* 2019 (11) (2019) 1–32.
- [59] J. Cogan, M. Kagan, E. Strauss, A. Schwartzman, Jet-images: computer vision inspired techniques for jet tagging, *Journal of High Energy Physics* 2015 (2) (2015) 1–16.
- [60] G. Louppe, K. Cho, C. Becot, K. Cranmer, Qcd-aware recursive neural networks for jet physics, *Journal of High Energy Physics* 2019 (1) (2019) 1–23.
- [61] L. de Oliveira, M. Paganini, B. Nachman, Learning particle physics by example: location-aware generative adversarial networks for physics synthesis, *Computing and Software for Big Science* 1 (1) (2017) 4.
- [62] M. Paganini, L. de Oliveira, B. Nachman, Accelerating science with generative adversarial networks: an application to 3d particle showers in multilayer calorimeters, *Physical review letters* 120 (4) (2018) 042003.
- [63] H. Kheddar, Y. Himeur, A. I. Awad, Deep transfer learning for intrusion detection in industrial control networks: A comprehensive review, *Journal of Network and Computer Applications* 220 (2023) 103760.
- [64] Y. Himeur, S. Al-Maadeed, H. Kheddar, N. Al-Maadeed, K. Abualsaud, A. Mohamed, T. Khattab, Video surveillance using deep transfer learning and deep domain adaptation: Towards better generalization, *Engineering Applications of Artificial Intelligence* 119 (2023) 105698.
- [65] H. Kheddar, Y. Himeur, S. Al-Maadeed, A. Amira, F. Bensaali, Deep transfer learning for automatic speech recognition: Towards better generalization, *Knowledge-Based Systems* 277 (2023) 110851.
- [66] A. Gueriani, H. Kheddar, A. C. Mazari, Deep reinforcement learning for intrusion detection in iot: A survey, in: *2023 2nd International Conference on Electronics, Energy and Measurement (IC2EM)*, Vol. 1, IEEE, 2023, pp. 1–7.
- [67] Y. Himeur, I. Varlamis, H. Kheddar, A. Amira, S. Atalla, Y. Singh, F. Bensaali, W. Mansoor, Federated learning for computer vision, *arXiv preprint arXiv:2308.13558* (2023).